

AD-754 959

TECHNOLOGY DEVELOPMENT FOR TRANSITION  
METAL-RARE EARTH HIGH-PERFORMANCE  
MAGNETIC MATERIALS

Joseph J. Becker

General Electric Corporate Research and  
Development

Prepared for:

Air Force Materials Laboratory  
Advanced Research Projects Agency

September 1972

DISTRIBUTED BY:

**NTIS**

National Technical Information Service  
U. S. DEPARTMENT OF COMMERCE  
5285 Port Royal Road, Springfield Va. 22151

AD 754959

TECHNOLOGY DEVELOPMENT FOR TRANSITION METAL-RARE  
EARTH HIGH-PERFORMANCE MAGNETIC MATERIALS

Contract No. F33615-70-C-1626

Sponsored by the Advanced Research Projects Agency

ARPA Order No. 1617, Program Code No. OD10

Contract effective date: 30 June 1970. Expiration date: 30 June 1973

Approved for public release;  
distribution unlimited.

Submitted to:

Air Force Materials Laboratory, AFSC, USAF  
Project Engineer: J. C. Olson, LPE, Tel. (513)255-4474

By:

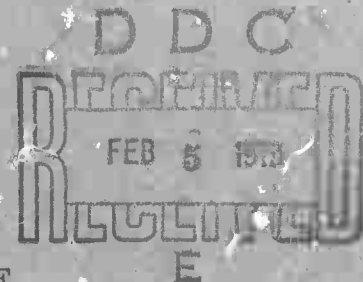
J. J. Becker, Principal Investigator, Tel. (518)346-8771, Ext. 6114  
GENERAL ELECTRIC COMPANY  
CORPORATE RESEARCH AND DEVELOPMENT  
P. O. Box 8  
SCHENECTADY, NEW YORK 12301

Reproduced by  
NATIONAL TECHNICAL  
INFORMATION SERVICE  
U S Department of Commerce  
Springfield VA 22151

The views and conclusions contained in this document are those of the authors and should not be interpreted as necessarily representing the official policies, either expressed or implied, of the Advanced Research Projects Agency or the U. S. Government.

Details of illustrations in  
this document may be better  
studied on microfiche

SRD-72-126



## NOTICE

When Government drawings, specifications, or other data are used for any purpose other than in connection with a definitely related Government procurement operation, the United States Government thereby incurs no responsibility nor any obligation whatsoever; and the fact that the government may have formulated, furnished, or in any way supplied the said drawings, specifications, or other data, is not to be regarded by implication or otherwise as in any manner licensing the holder or any other person or corporation, or conveying any rights or permission to manufacture, use, or sell any patented invention that may in any way be related thereto.



Copies of this report should not be returned unless return is required by security considerations, contractual obligations, or notice on a specific document.

## DOCUMENT CONTROL DATA - R &amp; D

(Security classification of title, body of abstract and indexing annotation must be entered when the overall report is classified)

## 1. ORIGINATING ACTIVITY (Corporate author)

General Electric Company  
Corporate Research and Development  
Schenectady, New York

## 2a. REPORT SECURITY CLASSIFICATION

Unclassified

## 2b. GROUP

## 3. REPORT TITLE

TECHNOLOGY DEVELOPMENT FOR TRANSITION METAL-RARE EARTH  
HIGH-PERFORMANCE MAGNETIC MATERIALS

## 4. DESCRIPTIVE NOTES (Type of report and inclusive dates)

Semiannual Interim Technical Report - January 1, 1972 to June 31, 1972

## 5. AUTHOR(S) (First name, middle initial, last name)

Joseph J. Becker

## 6. REPORT DATE

September 1972

## 7a. TOTAL NO. OF PAGES

88 53

## 7b. NO. OF REFS

88

## 8a. CONTRACT OR GRANT NO.

F33615-70-C-1626

## b. PROJECT NO.

ARPA Order No. 1617

## c.

Program Code No. OD10

## 9a. ORIGINATOR'S REPORT NUMBER(S)

SRD-72-126

## 9b. OTHER REPORT NO(S) (Any other numbers that may be assigned this report)

AFML-TR-72-187

## 10. DISTRIBUTION STATEMENT

Approved for public release; distribution unlimited.

## 11. SUPPLEMENTARY NOTES

Details of illustrations in  
this document may be better  
studied on microfiche

## 12. SPONSORING MILITARY ACTIVITY

Air Force Materials Laboratory (LPE)  
Wright-Patterson Air Force Base  
Ohio 45433

## 13. ABSTRACT

A session that has been organized for the 1972 Magnetism Conference will review work done under this contract and elsewhere on the problem of the origin of the coercive force in high-anisotropy materials. Polarized light metallography has been used to study magnetic domain configurations in  $\text{Co}_5\text{Sm}$ ,  $\text{Co}_5\text{Y}$ ,  $\text{Co}_5\text{Ce}$ , and  $\text{Co}_5\text{Pr}$  as a function of crystal thickness. From measurements of equilibrium domain widths on thin crystals, the domain wall energy in these compounds is estimated to be 85, 35, 25, and 40 ergs/cm<sup>2</sup> respectively. From surface domain wall observations on bulk crystals, crude estimates of wall energy have also been made for  $\text{Co}_5\text{Nd}$ ,  $\text{Co}_5\text{La}$ , and  $\text{Co}_5\text{Gd}$ . Magnetic domain structures in several  $\text{Co}_{17}\text{R}_2$ ,  $(\text{Co}, \text{Fe})_{17}\text{R}_2$ , and  $\text{Co}_7\text{R}_2$  phases have been examined using polarized light. Characteristic easy-axis domain patterns were seen in  $\text{Co}_{17}\text{Sm}_2$ ,  $\text{Co}_{17}\text{Gd}_2$ , and  $(\text{Co}, \text{Fe})_{17}\text{R}_2$  and  $\text{Co}_7\text{R}_2$  phases. Domains were not seen in  $\text{Co}_{17}\text{Pr}_2$ ,  $\text{Co}_{17}\text{Ce}_2$ ,  $\text{Co}_{17}\text{Y}_2$ , and  $\text{Co}_{17}\text{Nd}_2$ , all of which are believed to have easy-plane rather than easy-axis magnetic symmetry. The magnetic moment and hysteresis properties of a high-density, nearly completely oriented  $\text{Co}_5\text{Sm}$  magnet alloy up to 140 kOe. A saturation moment per gram of 98 G-cm<sup>3</sup>/g is measured at 300°K and shows a slight increase as temperature is decreased. After adjustment for voids and oxide the saturation moment per gram of the Co-Sm alloy is 102 G-cm<sup>3</sup>/g, or equivalent to 11,000 gauss for the saturation magnetization, 4 $\pi$ J<sub>s</sub>. An energy product of approximately 24 MGoe is attained at 300°K. The demagnetization properties of a series of sintered Co-Sm magnets have been measured over the range 0° to 750°K. The intrinsic coercive force of the samples varied from 19 to 65 kOe at 27°K, but decreased with increasing temperature to zero at about 700°K. The relative change of coercivity with temperature was the same for all the samples. Thus, it appears that the factors which influence the magnitude of coercivity do not influence the temperature dependence. Saturation magnetization, intrinsic coercive force, anisotropy field, and anisotropy constants were determined for a sample of sintered  $\text{Co}_5\text{Sm}$  at 4.2, 77, 300, and 500°K. The relationship between the temperature dependence of the coercivity and the anisotropy parameters is discussed.

14

KEY WORDS

LINK A

LINK B

LINK C

ROLE

WT

ROLE

WT

ROLE

WT

Magnetic Materials  
Permanent Magnets  
Cobalt-Rare Earth  
Magnetism

16

TECHNOLOGY DEVELOPMENT FOR TRANSITION METAL-RARE  
EARTH HIGH-PERFORMANCE MAGNETIC MATERIALS

J. J. Becker et al.

Approved for public release;  
distribution is unlimited.


## FOREWORD

This report describes work carried out in the Metallurgy and Ceramics Laboratory of the General Electric Research and Development Center, Schenectady, New York, under USAF Contract No. F33615-70-C-1626, entitled "Technology Development for Transition Metal-Rare Earth High-Performance Magnetic Materials." This work is administered by the Air Force Materials Laboratory, Wright-Patterson Air Force Base, Ohio, J. C. Olson (AFML/LPE), Project Engineer.

This Fourth Semiannual Interim Technical Report covers work conducted under the above program during the period 1 January - 30 June 1972. The principal participants in the research are J. J. Becker, J. D. Livingston, M. D. McConnell, J. G. Smeggil, S. Foner, E. J. McNiff, Jr., D. L. Martin, and M. G. Benz. The report was submitted by the author in July 1972.

The contractor's report number is

This technical report has been reviewed and is approved.

  
CHARLES E. EHRENFRIED  
Major, USAF  
Chief, Solid State Materials Branch  
Electromagnetic Materials Division  
Air Force Materials Laboratory

## ABSTRACT

A session that has been organized for the 1972 Magnetism Conference will review work done under this contract and elsewhere on the problem of the origin of the coercive force in high-anisotropy materials. Polarized light metallography has been used to study magnetic domain configurations in  $\text{Co}_5\text{Sm}$ ,  $\text{Co}_5\text{Y}$ ,  $\text{Co}_5\text{Ce}$ , and  $\text{Co}_5\text{Pr}$  as a function of crystal thickness. From measurements of equilibrium domain widths on thin crystals, the domain wall energy in these compounds is estimated to be 85, 35, 25, and 40 ergs/cm<sup>3</sup> respectively. From surface domain wall observations on bulk crystals, crude estimates of wall energy have also been made for  $\text{Co}_5\text{Nd}$ ,  $\text{Co}_5\text{La}$ , and  $\text{Co}_5\text{Gd}$ . Magnetic domain structures in several  $\text{Co}_{17}\text{R}_2$ ,  $(\text{Co}, \text{Fe})_{17}\text{R}_2$ , and  $\text{Co}_7\text{R}_2$  phases have been examined using polarized light. Characteristic easy-axis domain patterns were seen in  $\text{Co}_{17}\text{Sm}_2$ ,  $\text{Co}_{17}\text{Gd}_2$ , and  $(\text{Co}, \text{Fe})_{17}\text{R}_2$  and  $\text{Co}_7\text{R}_2$  phases. Domains were not seen in  $\text{Co}_{17}\text{Pr}_2$ ,  $\text{Co}_{17}\text{Ce}_2$ ,  $\text{Co}_{17}\text{Y}_2$ , and  $\text{Co}_{17}\text{Nd}_2$ , all of which are believed to have easy-plane rather than easy-axis magnetic symmetry. The magnetic moment and hysteresis properties of a high-density, nearly completely oriented  $\text{Co}_5\text{Sm}$  magnet alloy have been measured from 300°K to 4.2°K and in applied fields up to 140 kOe. A saturation moment per gram of 98 G-cm<sup>3</sup>/g is measured at 300°K and shows a slight increase as temperature is decreased. After adjustment for voids and oxide the saturation moment per gram of the Co-Sm alloy is 102 G-cm<sup>3</sup>/g, or equivalent to 11,000 gauss for the saturation magnetization,  $4\pi J_s$ . An energy product of approximately 24 MGOe is attained at 300°K. The demagnetization properties of a series of sintered Co-Sm magnets have been measured over the range 0° to 750°K. The intrinsic coercive force of the samples varied from 19 to 65 kOe at 27°K, but decreased with increasing temperature to zero at about 700°K. The relative change of coercivity with temperature was the same for all the samples. Thus, it appears that the factors which influence the magnitude of coercivity do not influence the temperature dependence. Saturation magnetization, intrinsic coercive force, anisotropy field, and anisotropy constants were determined for a sample of sintered  $\text{Co}_5\text{Sm}$  at 4.2, 77, 300, and 500°K. The relationship between the temperature dependence of the coercivity and the anisotropy parameters is discussed.

## TABLE OF CONTENTS

<u>Section</u>	<u>Page</u>
I INTRODUCTION - - - - -	1
II FUNDAMENTAL STUDIES OF THE ORIGIN OF THE COERCIVE FORCE IN HIGH-ANISOTROPY MATERIALS-	1
1. Origin of the coercive force (J. J. Becker) - - - - -	1
2. Domain-Wall Energy in Cobalt-Rare Earth Compounds (J. D. Livingston and M. D. McConnell) (Submitted to the Journal of Applied Physics) - - - - -	1
3. Magnetic Domains in $\text{Co}_{17}\text{R}_2$ , $(\text{Co}, \text{Fe})_{17}\text{R}_2$ , and $\text{Co}_7\text{R}_2$ Compounds (J. D. Livingston) (Submitted to the Journal of Materials Science) - - - - -	1
III MATERIALS CHARACTERIZATION AND PHASE EQUILIBRIUM STUDIES - - - - -	3
1. Summary of analytical results by wet chemistry and x-ray fluorescence spectroscopy (J. G. Smeggil) - - - -	3
IV ALLOY DEVELOPMENT - - - - -	1
1. Magnetic Properties of Cobalt-Samarium with a 24 MGOe Energy Product (S. Foner, E. J. McNiff, D. L. Martin, and M. G. Benz) (Applied Physics Letters, Vol. 20, No. 11, 1 June 1972, p. 447) - - - - -	1
2. Temperature Variation of Coercivity for Co-Sm Permanent Magnet Alloys (D. L. Martin and M. G. Benz) (1972 Intermag Conference. Submitted to IEEE Trans- actions on Magnetics) - - - - -	1
3. Anisotropy Parameters and Coercivity for Sintered $\text{Co}_5\text{Sm}$ Permanent Magnet Alloys (M. G. Benz and D. L. Martin) (Submitted to Applied Physics Letters)- - - - -	1

# LIST OF ILLUSTRATIONS

Section		Page
II-2	<u>Domain-Wall Energy in Cobalt-Rare Earth Compounds</u>	
	Fig. 1 Magnetic domain patterns in a thin $\text{Co}_5\text{Sm}$ crystal after polishing to thicknesses of (a) $74\mu$ , (b) $24\mu$ , (c) $16\mu$ , (d) $16\mu$ , after application of normal magnetic field; and (e) $13\mu$ , (f) $13\mu$ , after field. Magnetic easy-axis normal to surface - - - - -	2
	Fig. 2 Magnetic domains in $\text{Co}_5\text{Y}$ at thicknesses of (a) $63\mu$ , (b) $30\mu$ , (c) $18\mu$ , (d) $15\mu$ , (e) $10\mu$ , after field - - - -	3
	Fig. 3 Magnetic domains in $\text{Co}_5\text{Ce}$ at thicknesses of (a) $96\mu$ , (b) $38\mu$ , (c) $18\mu$ , (d) $18\mu$ , after field; and (e) $10\mu$ , (f) $10\mu$ , different area - - - - -	4
	Fig. 4 Magnetic domains in $\text{Co}_5\text{Pr}$ at thicknesses of (a) $84\mu$ , (b) $33\mu$ , (c) $23\mu$ , after field; and (d) $13\mu$ , after field - - - - -	5
	Fig. 5 Domain patterns in bulk samples of (a) $\text{Co}_5\text{Nd}$ , (b) $\text{Co}_5\text{La}$ , and (c) $\text{Co}_5\text{Gd}$ - - - - -	6
	Fig. 6 Average internal domain width $W$ vs thickness $T$ for $\text{Co}_5\text{Y}$ . Theory predicts a shift from $T^{1/2}$ to $T^{2/3}$ dependence at $T_2 = 32\gamma/M_S^2$ . Calculated $T_2$ marked with arrow on abscissa - - - - -	8
II-3	<u>Magnetic Domains in <math>\text{Co}_{17}\text{R}_2</math>, <math>(\text{Co}, \text{Fe})_{17}\text{R}_2</math>, and <math>\text{Co}_7\text{R}_2</math> Compounds</u>	
	Fig. 1 Magnetic domains in $\text{Co}_{17}\text{Sm}_2$ . Rosette structure in grain at right is characteristic of easy-axis magnetic symmetry (photograph from J. J. Becker) - -	2
	Fig. 2 Easy-axis domain patterns in (a) $(\text{Co}_{0.75}\text{Fe}_{0.25})_{17}\text{Sm}_2$ , (b) $(\text{Co}_{0.6}\text{Fe}_{0.4})_{17}\text{Pr}_2$ - - - - -	2
	(c) $(\text{Co}_{0.7}\text{Fe}_{0.3})_{17}\text{Y}_2$ , (d) $(\text{Co}_{0.75}\text{Fe}_{0.25})_{17}\text{Ce}_2$ - - - -	3
	(e) $(\text{Co}_{0.7}\text{Fe}_{0.3})\text{Gd}_2$ - - - - -	3
	Fig. 3 Domain patterns in mechanically polished $\text{Co}_{17}\text{Gd}_2$ . These maze patterns are believed to be caused by surface strains - - - - -	4
	Fig. 4 Easy-axis domain patterns in (a) $\text{Co}_7\text{Sm}_2$ , (b) $\text{Co}_7\text{Pr}_2$ - - - - -	4
	(c) $\text{Co}_7\text{Y}_2$ , and (d) $\text{Co}_7\text{Nd}_2$ - - - - -	5

## List of Illustrations (continued)

<u>Section</u>		<u>Page</u>
II-3	Fig. 5 Magnetic domains in $\text{Co}_7\text{Gd}_2$ (a) before and (b) after touching sample with a magnet. Note downward motion of domain wall at right center and disappearance of dark domain at lower left. Domains are large because of low magnetic moment - - - - -	6
III-1	<u>Materials Characterization and Phase Equilibrium Studies</u>	
	Fig. 1 Comparison of analytical data from two sources on series of Co-Sm alloys - - - - -	4
	Fig. 2 X-ray fluorescence intensity ratio data taken on four samples on two different days - - - - -	5
IV	<u>Alloy Development</u>	
	Fig. 1 Magnetic moment, $\sigma$ , vs applied field $H_{\text{APP}}$ , for a small disk of Co-Sm magnet. The high degree of alignment is evidenced by saturation above 80 kOe - - - - -	2
	Fig. 2 Comparison of test results obtained on a long sintered bar as measured at the GE Magnetic Materials Product Section, Edmore, Mich., and CR&D with results measured on a disk at MIT - - - -	3
	<u>Temperature Variation of Coercivity for Co-Sm Permanent Magnet Alloys</u>	
	Fig. 1 Variation of demagnetization characteristics of a Co-Sm magnet with measurement temperature - - -	1
	Fig. 2 Change of intrinsic coercive force with temperature for a series of Co-Sm magnet samples. The data for the powder are from McCurrie <sup>(2)</sup> - - - - -	2
	Fig. 3 Relative coercivity vs temperature. The data in Fig. 2 have been normalized so that the relative coercivity at 77°K is 1 - - - - -	2
	<u>Anisotropy Parameters and Coercivity for Sintered <math>\text{Co}_5\text{Sm}</math> Permanent Magnet Alloys</u>	
	Fig. 1 Relative coercivity vs temperature. The data were normalized so that the relative coercivity at 77°K was equal to 1 - - - - -	9

# List of Illustrations (continued)

<u>Section</u>	<u>Page</u>
Fig. 2 Magnetization of the sample measured perpendicular to the c-axis as a function of field applied perpendicular to the c-axis- - - - -	10
Fig. 3 $H/J$ vs $J^2$ . The intercept is equal to $2K_1/J_S^2$ - - - -	10
Fig. 4 $H_{Ci}$ vs the anisotropy constant $K_1$ - - - - -	11
Fig. 5 $H_{Ci}$ vs the anisotropy field $H_A$ - - - - -	11
Fig. 6 $H_{Ci}$ vs the domain wall energy $\gamma$ divided by the saturation magnetic moment per unit volume $J_S$ - -	12
Fig. 7 $J_S(T)/J_S(0)$ and $K_1(T)/K_1(0)$ as a function of $T/T_C$ . $J_S(0)$ was taken as the value for $J_S$ at 4.2°K. $K_1(0)$ was taken as $K_1(77^\circ K)/0.889$ , the value 0.889 being $[1-T/T_C][J_S(T)/J_S(0)]^3$ at $T = 77^\circ K$ . The solid curve was calculated by placing the empirically determined Carr <sup>(16)</sup> type factor $(1-T/T_C)$ into the Zener <sup>(15)</sup> equation. $T_C$ was taken as 984°K. <sup>(7)</sup> - - - - -	12

# TECHNOLOGY DEVELOPMENT FOR TRANSITION METAL-RARE EARTH HIGH-PERFORMANCE MAGNETIC MATERIALS

J. J. Becker

## I. INTRODUCTION

This is the fourth semiannual interim technical report for Contract No. F33615-70-C-1626, covering the period 1 January 1972 through 30 June 1972. The objective of this work, as set forth in Exhibit A of the contract, is to develop the technology of high-performance transition metal-rare earth magnets for critical applications. High-performance permanent magnets are defined in this context as those having remanences greater than ten thousand gauss and permeabilities of very nearly unity throughout the second and into the third quadrants of their hysteresis loop. Such technology is to be developed through 1) studies of the origin of the intrinsic coercive force in high-anisotropy materials, 2) development of information on phase equilibria in these materials, and 3) identification and investigation of new materials. The progress that has been made during the period covered by this report is described below under these three major headings. Five of the sections of this report consist of papers that have been published or submitted for publication in various technical journals, as detailed in the Table of Contents.

## II. FUNDAMENTAL STUDIES OF THE ORIGIN OF THE COERCIVE FORCE IN HIGH-ANISOTROPY MATERIALS

### 1. Origin of the coercive force (J. J. Becker)

During the course of this contract, many experiments have been performed, and speculations indulged in, related to the origin of the coercive force in high-anisotropy materials, primarily of course the cobalt-rare-earths. Work by other investigators relating to this problem has also been under way, sometimes with results that appear consistent with the measurements and ideas that have been described in this contract, sometimes not. A single example of an unresolved inconsistency is the temperature dependence of the coercive force. Measurements of the coercive force of  $\text{Co}_5\text{Sm}$  particles, and also of  $\text{Co}_5\text{Sm}$  sintered magnets, show a fairly substantial and regular increase with falling temperature. Measurements of the nucleating field for individual jumps in single particles show a similar strong monotonic temperature dependence. On the other hand, measurements of the anisotropy constants of  $\text{Co}_5\text{Sm}$  single crystals reported by Tatsumoto show a broad peak at about  $180^\circ\text{K}$ , with the anisotropy decreasing at both higher and lower temperature. Thus far, this need not be inconsistent with the developing concept of imperfection-controlled nucleation of magnetization reversal, which implies that the observed temperature dependence of  $H_c$  or  $H_n$  will be that of the relevant nucleus, not the bulk constants of the parent material. On the other hand, as described

later in this report, Benz and Martin have been measuring both  $H_c$  and  $K$  on the same samples of sintered  $\text{Co}_5\text{Sm}$  and find that they vary in the same way. The  $K$  of this material appears to increase regularly with decreasing temperature, in contrast to Tatsumoto's measurements. Here is a clear discrepancy, unless the  $K$  of sintered magnets really is substantially different from that of as-cast material, which would be remarkable enough. First-hand discussions by the author with Professor Tatsumoto and his group at the time of the IEEE Intermag Conference in Kyoto established that the composition of the single crystals were not determined, and that the anisotropy measurements were made by extrapolation of hard-direction magnetization curves from a maximum field of only 16 kOe. It seems fair to regard the single-crystal values as less than definitively established. Furthermore, there are indications from work reported by Westendorp at last year's Magnetism Conference that the domain wall energy in cast material rises with decreasing temperature in the same way as the coercive force. The domain wall energy must be determined by the bulk constants only. What, then, are the bulk constants of  $\text{Co}_5\text{Sm}$ ? How do they vary with temperature? How do they vary with composition? Are there any other variables that must be controlled in order to be able to make reproducible anisotropy constant measurements? How do single crystals compare with oriented sintered materials? The situation needs definitive experiments.

During the time of the present report, the author has organized a session on the origin of the coercive force in high-anisotropy materials, to be held at the forthcoming 18th Annual Conference on Magnetism and Magnetic Materials in November 1972. This appears to be a propitious time to review carefully the present understanding of this problem on both the theoretical and experimental levels, in both powders and sintered aggregates.

The session will consist of a paper reviewing the present status of the problem, given by J. D. Livingston of the General Electric Research and Development Center, followed by a panel discussion. The panel members include K. J. Strnat, University of Dayton; R. A. McCurrie, University of Bradford; K. Bachmann, Brown-Boveri; and G. Y. Chin, Bell Laboratories. The purpose of the session will be to pinpoint as precisely as possible where the understanding of the problem stands, what discrepancies exist, and what exactly should be done next to advance the understanding of this subject most effectively, thereby establishing the strongest possible base for continued development of this class of materials.

# DOMAIN-WALL ENERGY IN COBALT-RARE EARTH COMPOUNDS

J. D. Livingston and M. D. McConnell  
(Submitted to the Journal of Applied Physics)

## INTRODUCTION

The cobalt-rare earth compounds, especially  $\text{Co}_5\text{Sm}$ , provide the basis for a new class of permanent magnet materials with coercive forces and energy products significantly higher than those of previous magnet materials. (1-3) These compounds possess a large magnetocrystalline anisotropy of uniaxial symmetry. Coercive force appears to be controlled by the nucleation and pinning of magnetic domain walls. (1, 4)

Such mechanisms depend on the energy per unit area of a domain wall, and observations by Westendorp(5) indicate that this quantity may be larger for  $\text{Co}_5\text{Sm}$  than for other  $\text{Co}_5\text{R}$  compounds ( $\text{R}$  = rare earth, La, or Y). He suggested that this may explain why high coercive forces are easily attained in  $\text{Co}_5\text{Sm}$ , but not in most of the other compounds.

There has been considerable study of the domain structures of uniaxial ferromagnetic materials. (6-8) Of particular interest are the domain structures in thin plates in which the magnetic easy axis is normal to the face of the plate. Theory for these structures is well developed, and allows determination of domain-wall energies by measurements of domain widths. Although several observations of domain patterns in  $\text{Co}_5\text{R}$  compounds have been reported in the literature (Ref. 5, 9-12), no domain-wall energy measurements have been made. We report below the results of such measurements.

## EXPERIMENTAL

The compounds were prepared by arc-casting from high-purity materials and annealed for 24 hours at  $1100^\circ\text{C}$  (or, for  $\text{Co}_5\text{La}$ , at  $1000^\circ\text{C}$ ) for homogenization and grain growth.

Samples were initially mounted in epoxy resin and vacuum impregnated. After curing, the mounted sample was ground and polished on one face. This face was examined under polarized light to locate a suitable grain of satisfactory size and orientation. We used a Bausch and Lomb metallograph with an elliptical compensator to optimize the optical contrast. (13) After mapping the location of the grain, the polished face was cemented with clear epoxy to a cleaned glass petrographic slide. The mounted sample was placed in a vacuum chuck and most of the sample was removed with a precision saw. With a special petrographic slide holder, the sample was ground to a thickness of about  $75\mu$  on a rotating lap. Sample thickness was monitored by micrometer, allowing for the thickness of the glass slide and epoxy cement.

Micrographs were then taken in polarized light

of the original polished surface of the chosen grain. Thinning of the sample was continued by hand polishing on bond paper with  $6\mu$  diamond paste or, in the later stages,  $3\mu$  diamond paste. At suitable intervals the thickness was monitored and the grain photographed. Average width of magnetic domains was measured from micrographs at 500X magnification. When the sample was approximately  $10\mu$  thick, the sample and glass slide were mounted on edge in epoxy. They were ground until the grain was intercepted and an accurate measurement of the sample thickness could be made on the metallographic microscope. This allowed calibration of the thicknesses measured by micrometer.

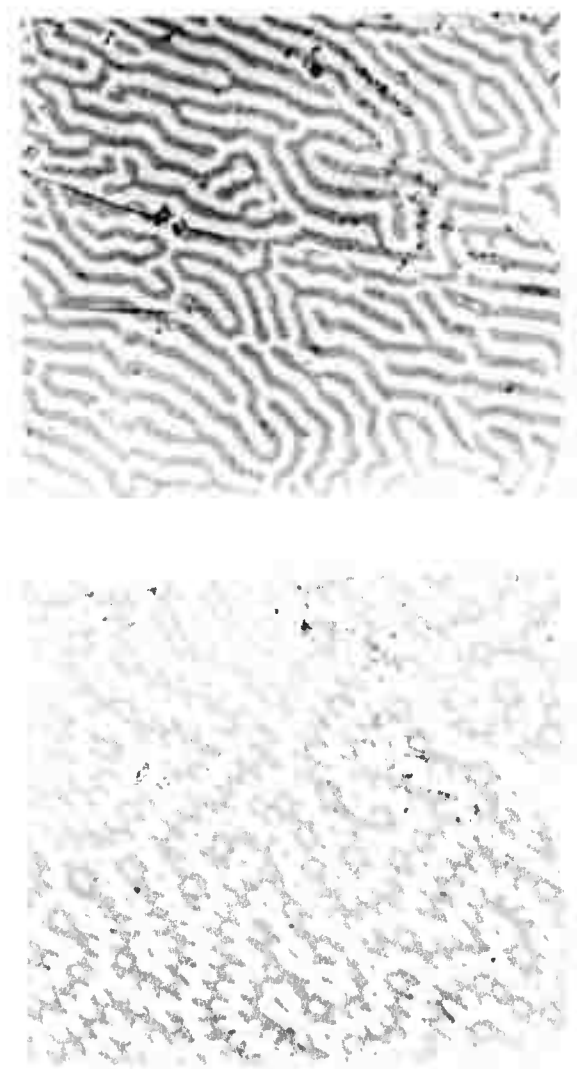
## OBSERVATIONS

The qualitative observations were consistent with earlier observations on  $\text{Co}_5\text{R}$  (5, 9-12) and other easy-axis materials. (6-8) In most grains, the easy-axis had a substantial component within the surface plane, and domain patterns were elongated in this direction. For our measurements, however, we were interested in grains with the easy-axis nearly normal to the surface, which are recognizable by characteristic patterns such as seen in  $\text{Co}_5\text{Sm}$  in Fig. 1(a).

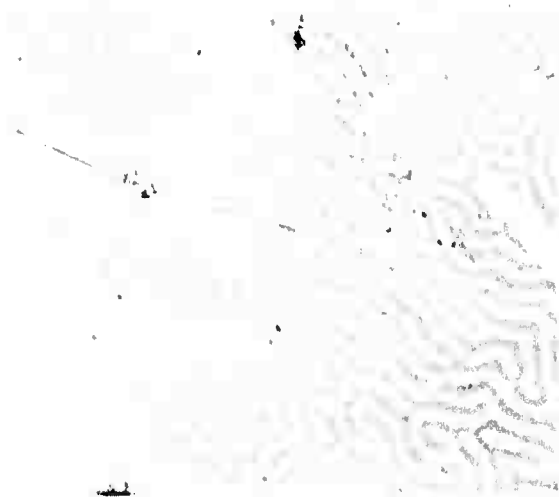
To reduce magnetostatic energy, the simple maze domain structures that are present in the interior of the crystal are refined in the vicinity of the surface. This surface domain refinement has two distinct features: extreme corrugations and the introduction of reverse "spike" domains visible as small spots in Fig. 1(a). When the crystal is thinned sufficiently, such surface refinement can no longer occur, and the simple maze structure extends throughout the thickness. Thus, the domain patterns observed gradually simplify as thickness is reduced, as seen in Figs. 1(b) through (f). Qualitative observations for  $\text{Co}_5\text{Y}$ ,  $\text{Co}_5\text{Ce}$ , and  $\text{Co}_5\text{Pr}$  are similar, as shown in Figs. 2 through 4.

To see how well the domain structures approach equilibrium, domains were occasionally removed by saturating the magnetization with a field of 20,000 Oe normal to the surface and then removing the field to allow re-nucleation of the domains. Domain patterns were photographed before and after this process, and examples of the changes produced are seen by comparing Figs. 1(c) and 1(d), 1(e) and 1(f), 2(e) and 2(f), and 3(c) and 3(d).

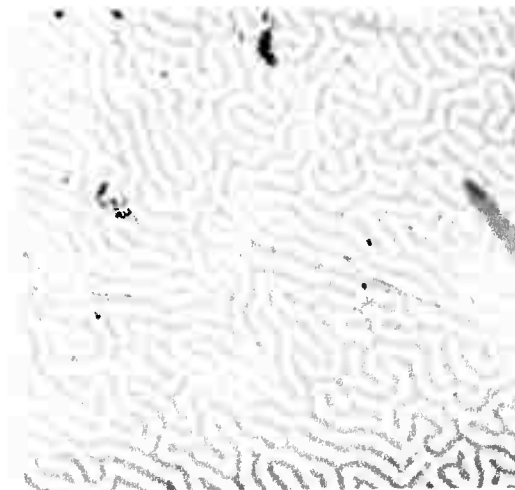
We also found characteristic easy-axis domain patterns in samples of  $\text{Co}_5\text{Nd}$ ,  $\text{Co}_5\text{La}$ , and  $\text{Co}_5\text{Gd}$  (Fig. 5). The optical contrast was rather faint in  $\text{Co}_5\text{Nd}$  and  $\text{Co}_5\text{La}$ , and domain motion and nucleation were found to be very restricted in  $\text{Co}_5\text{Gd}$ . The domains in Fig. 5(c) showed no change after slight



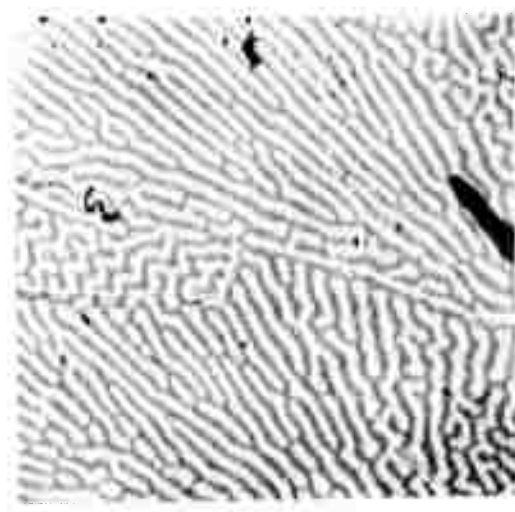
(a)



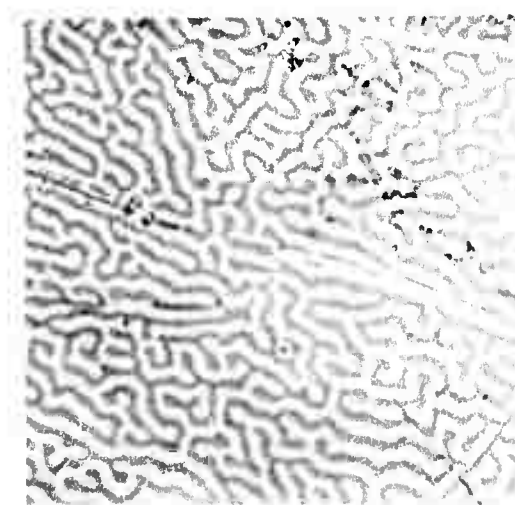
(b)



(c)



(d)



(e)

Fig. 1 Magnetic domain patterns in a thin  $\text{Co}_5\text{Sm}$  crystal after polishing to thicknesses of (a)  $74\mu$ , (b)  $24\mu$ , (c)  $16\mu$ , (d)  $16\mu$ , after application of normal magnetic field; and (e)  $13\mu$ , (f)  $13\mu$ , after field. Magnetic easy-axis normal to surface.

375X

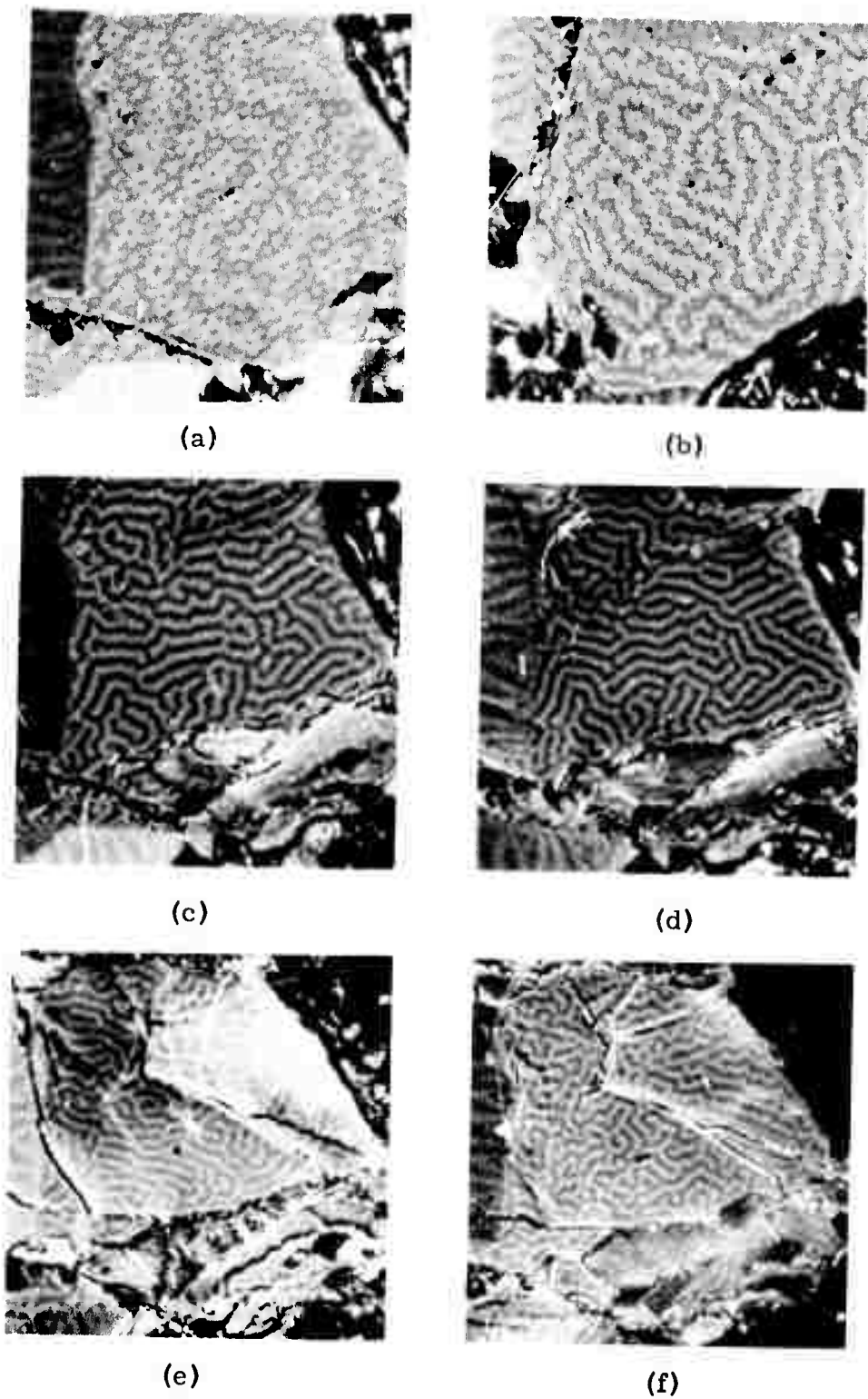
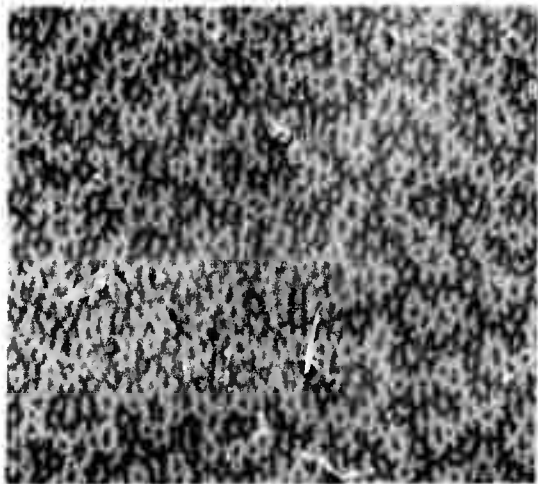
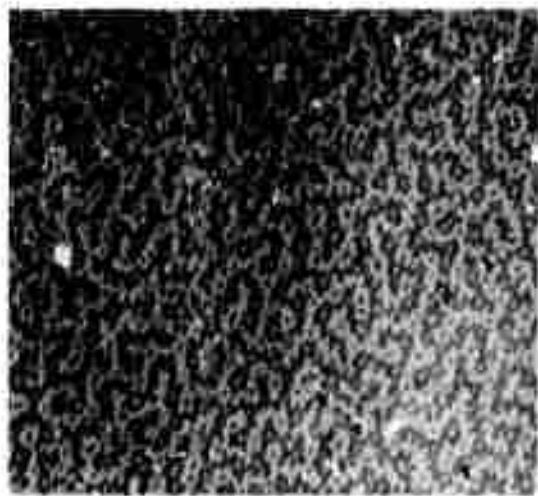


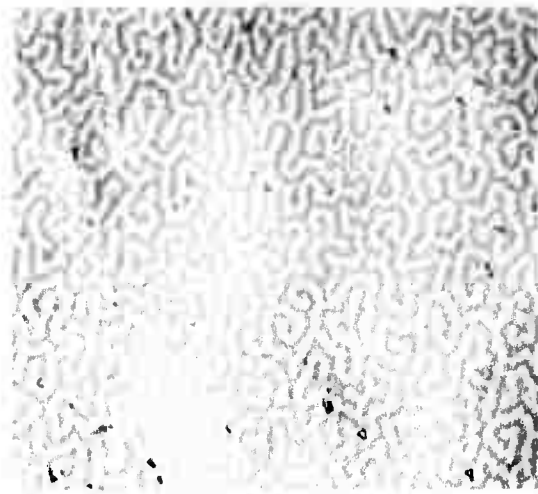
Fig. 2 Magnetic domains in Co<sub>5</sub>Y at thicknesses of (a) 63μ, (b) 30μ, (c) 18μ, (d) 15μ, (e) 10μ, and (f) 10μ, after field. 500X



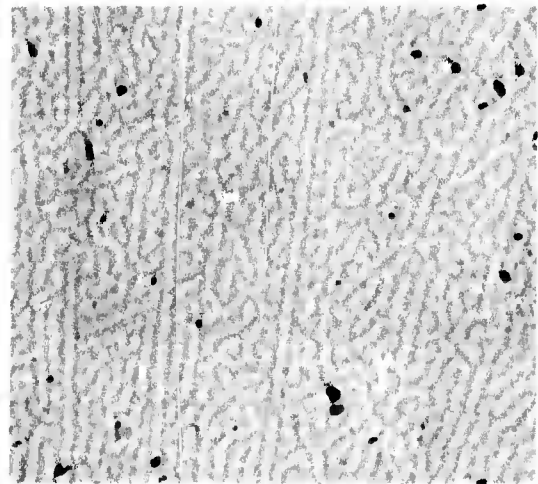
(a)



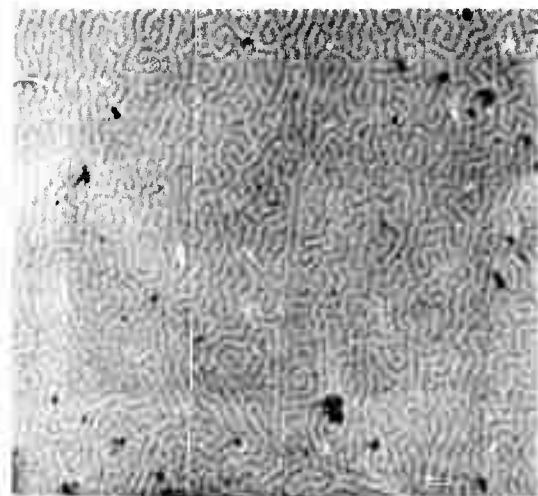
(b)



(c)



(d)



(e)



(f)

Fig. 3 Magnetic domains in  $\text{Co}_3\text{Ce}$  at thicknesses of (a)  $96\mu$ , (b)  $38\mu$ , (c)  $18\mu$ , (d)  $18\mu$ , after field; and (e)  $10\mu$ , (f)  $10\mu$ , different area. 375X

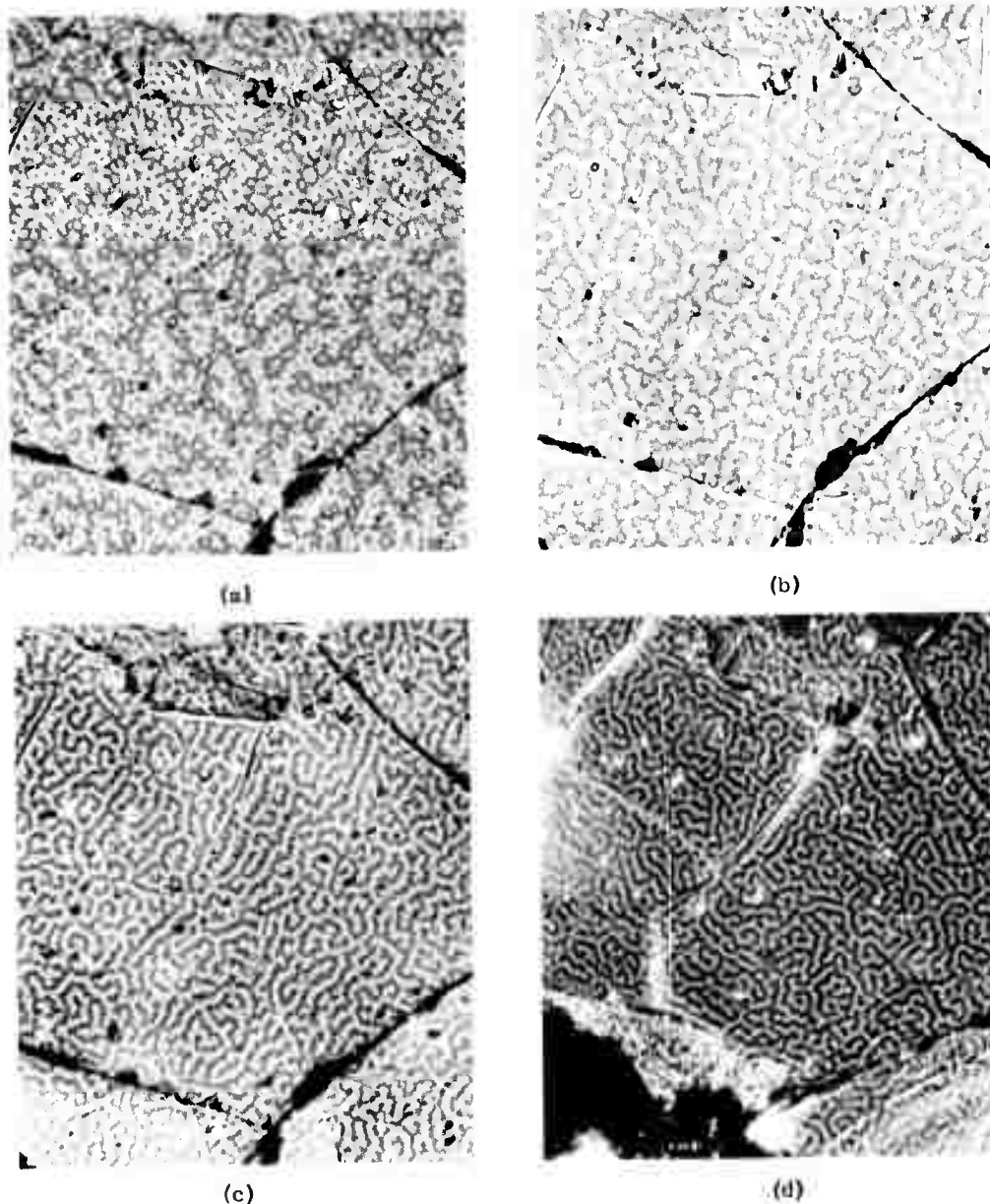


Fig. 4 Magnetic domains in  $\text{Co}_5\text{Pr}$  at thicknesses of (a)  $84\mu$ , (b)  $33\mu$ , (c)  $23\mu$ , after field; and (d)  $13\mu$ , after field. 375X

thinning, and when they were removed by magnetizing in 20,000 Oe, domains did not re-nucleate on returning to zero field. ] We therefore decided not to initiate the tedious thinning process for these three compounds.

#### WALL ENERGY DETERMINATION

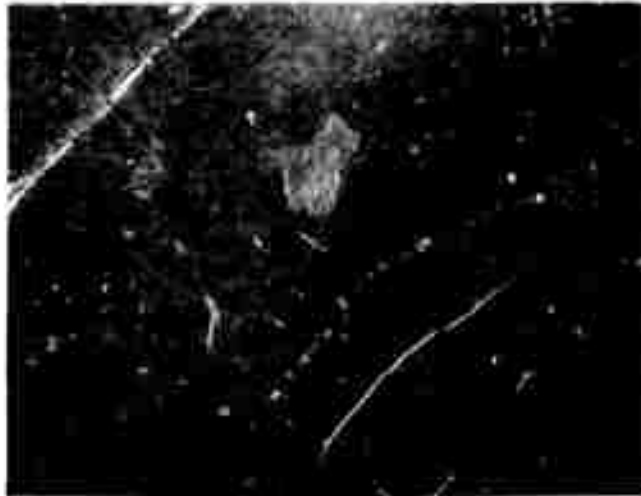
Kittel(14) considered the equilibrium domain structure of a high-anisotropy ferromagnetic plate of thickness  $T$  with the easy-axis normal to the plate. The total energy per unit area of an array of parallel plate domains of width  $W$  is the sum of the magneto-static energy,  $1.7 M_s^2 W$ , and the domain-wall energy,

$\gamma T/W$ . (Here  $M_s$  is the magnetic moment per unit volume and  $\gamma$  is the domain-wall energy per unit area of wall.) The equilibrium domain width is obtained by minimizing this total energy, which yields

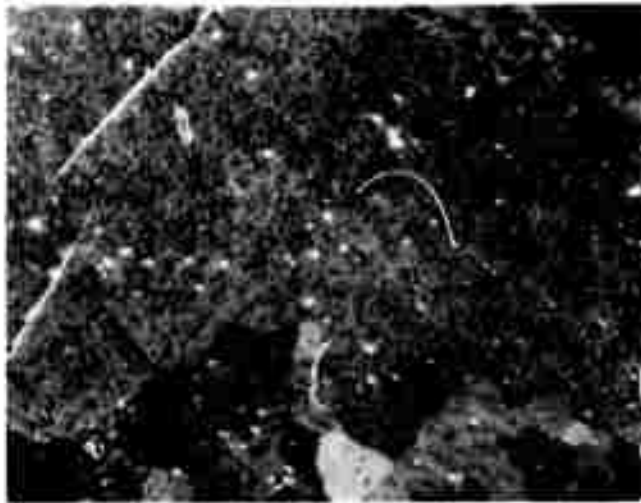
$$W = (\gamma T / 1.7 M_s^2)^{1/2} \quad (1)$$

Hence if  $M_s$  is known,  $\gamma$  can be determined by measuring  $W$  at a given  $T$ .

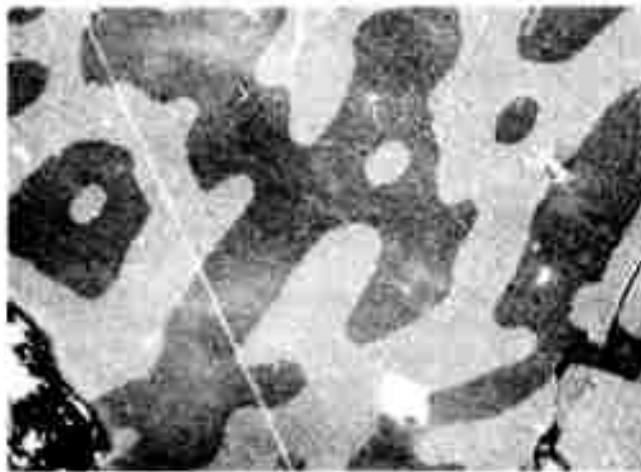
Several questions arise concerning the application of Eq. (1) and Kittel's simple model to our results. First, although regions of parallel plates are



(a)



(b)



(c)

Fig. 5 Domain patterns in bulk samples of (a)  $\text{Co}_5\text{Nd}$  (750X), (b)  $\text{Co}_5\text{La}$  (375X), and (c)  $\text{Co}_5\text{Gd}$  (375X).

TABLE I  
Equilibrium Domain Widths and Domain-Wall Energies of  $\text{Co}_5\text{R}$  Compounds

Material	Saturation Magnetization <sup>(3)</sup> $M_s$ (emu)	Thickness $T$ ( $\mu$ )	Average Domain Width $W$ ( $\mu$ )	Domain-Wall Energy $\gamma$ (ergs/cm <sup>2</sup> )
$\text{Co}_5\text{Sm}$ Grain A	855	6	2.1	90
		6	2.0*	83
		14	3.3	92
		13	3.0	86
		13	2.8*	74
		16	3.2	79
		16	3.2*	79
		19	3.5	79
		24	4.0	83
$\text{Co}_5\text{Y}$	848	10	1.7	35
		10	1.7*	35
		15	2.0	33
		18	2.2	33
$\text{Co}_5\text{Ce}$	615	10	1.9	23
		10	1.9*	23
		18	2.8*	28
$\text{Co}_5\text{Pr}$	960	13	1.9	44
		13	1.8*	40
		23	2.4*	39
$\text{Co}_5\text{Nd}$	983	--		( $\approx 20$ )
$\text{Co}_5\text{La}$	725	--		( $\approx 30$ )
$\text{Co}_5\text{Gd}$	287	--		( $\approx 30?$ )

\* After application of field.

sometimes seen [Fig. 3(f)], we commonly observe maze structures. Fortunately, maze and parallel plate structures of the same width have nearly the same energy, so this difference is unimportant. (6) Second is the question of how closely equilibrium is achieved. Since the removal and re-nucleation of domains by the application and removal of a field usually resulted in a demagnetized sample with nearly the same average domain width, it is felt that equilibrium is closely approached in these materials (with the exception of  $\text{Co}_5\text{Gd}$ ).

Several theoretical limitations to Eq. (1) have been discussed by Kaczer. (6) Deviation of the magnetization direction from the easy-axis direction, the so-called  $\mu^*$  effect, is important in some materials but is negligible in these high-anisotropy materials. Below a thickness of about  $T_1 = \gamma/2M_s^2$ , the magnetostatic interaction between top and bottom surfaces becomes important, and the equilibrium  $W$  goes through a minimum and begins to increase with decreasing  $T$ . This limitation is not important in our experiments because we always have  $T \gg T_1$ . More important to

our experiments is the upper thickness limit for the validity of Eq. (1), which Kaczer<sup>(6)</sup> gives approximately as  $T_2 = 32\gamma/M_s^2$ . This marks the thickness at which surface refinement of the domain structure begins to appear, usually by the appearance of corrugations and spike domains. For  $T > T_2$ , the equilibrium internal domain width now increases more rapidly, as  $T^{2/3}$ . (6,15) However, theory predicts an average surface domain width that eventually becomes independent of thickness and proportional to  $\gamma/M_s^2$ . (15)

We have tabulated in Table I our data for equilibrium domain width  $W$  for thicknesses where spike domains and corrugations had essentially disappeared, i. e., for  $T < T_2$ . Each value of  $W$  is the average of at least 20 measurements. Since Eq. (1) is valid in this regime, we have calculated from each  $W$  a value of domain-wall energy  $\gamma$ , and averaged these for each compound. In view of the inaccuracies in our measurements of  $W$  and  $T$ , and possible slight departure from equilibrium in some cases, we estimate the values of  $\gamma$  listed in Table I to be accurate to  $\pm 15\%$ .

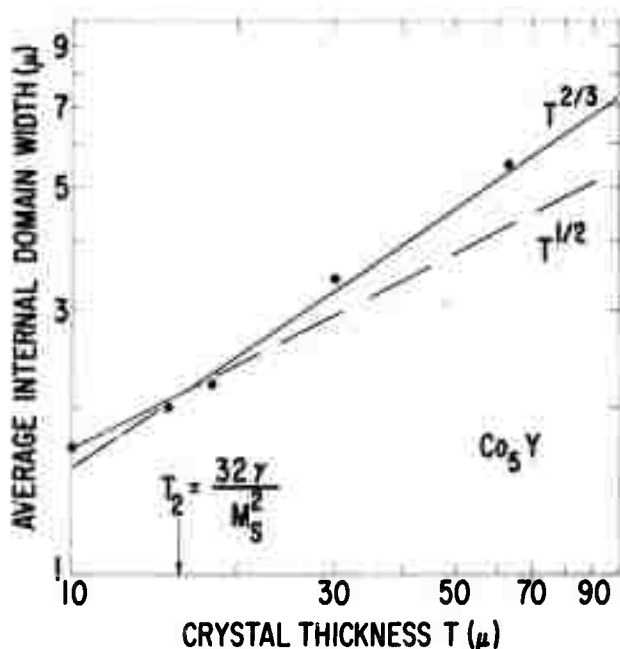


Fig. 6 Average internal domain width  $W$  vs thickness  $T$  for  $\text{Co}_5\text{Y}$ . Theory predicts a shift from  $T^{1/2}$  to  $T^{2/3}$  dependence at  $T_2 = 32\gamma/M_s^2$ . Calculated  $T_2$  marked with arrow on abscissa.

For thicknesses  $T > T_2$ , the internal domain width can be measured from surface domain patterns by ignoring corrugations and spike domains. Data for  $\text{Co}_5\text{Y}$ , shown in Fig. 6, demonstrate the shift from  $T^{1/2}$  to  $T^{2/3}$  dependence predicted by theory. By Kaczer's formula, this dependence should change at  $T_2 = 16\mu$ , in reasonable agreement with Fig. 6.

According to theory,<sup>(15)</sup> the surface domain width at large thicknesses is constant and could also be used as a measure of  $\gamma$ . Surface domain patterns are more complex than considered by theory, and it is not clear just what should be measured. However, for semiquantitative estimates of  $\gamma$ , it may be satisfactory to measure some characteristic distance, such as average wavelength  $\lambda$  of corrugations. On thick samples of  $\text{Co}_5\text{Gd}$ ,  $\text{Co}_5\text{Sm}$ ,  $\text{Co}_5\text{Ce}$ ,  $\text{Co}_5\text{Y}$ ,  $\text{Co}_5\text{La}$ ,  $\text{Co}_5\text{Pr}$ , and  $\text{Co}_5\text{Nd}$ , we measured  $\lambda = 30\mu$ ,  $6\mu$ ,  $4\mu$ ,  $3.5\mu$ ,  $3.5\mu$ ,  $3\mu$ , and  $1.5\mu$ , respectively. Use of comparative  $\lambda M_s^2$  values as a rough measure of comparative  $\gamma$  values led to the estimates for  $\text{Co}_5\text{Nd}$ ,  $\text{Co}_5\text{La}$ , and  $\text{Co}_5\text{Gd}$  listed in Table I. The estimate for  $\text{Co}_5\text{Gd}$  should be considered as particularly questionable because of the evidence discussed earlier of nonequilibrium domain behavior in this material.

## DISCUSSION

The wall energies listed in Table I are the highest yet measured for any material. [For comparison,  $\gamma = 1 - 5 \text{ erg/cm}^2$  for various ferrites<sup>(6, 8)</sup> and

$\gamma = 11 \text{ ergs/cm}^2$  for cobalt.<sup>(6)</sup>] This was expected, because the wall energy depends on the magneto-crystalline anisotropy constant  $K$ , which is extremely high for these compounds. The standard continuum model of a domain wall yields the formula:<sup>(7)</sup>

$$\gamma = 4(AK)^{1/2} \quad (2)$$

where  $A$  is the exchange constant.

We have listed in Table II our measured values of  $\gamma$  and values of  $K$  from single-crystal measurements by Tatsumoto et al.<sup>(16)</sup> The qualitative correlation is good. From these values and Eq. (2), we have calculated values for  $A$  and listed them in Table II. [For comparison,  $A = 3 \times 10^{-6} \text{ ergs/cm}$  for hexagonal cobalt.<sup>(17, 18)</sup>] The exchange constant  $A$  for  $\text{Co}_5\text{Sm}$  appears to be significantly higher than for the other compounds. However, for reasons discussed in the next two paragraphs, the validity of Eq. (2) for these materials is questionable.

The exchange constant  $A$  is sometimes<sup>(19)</sup> approximated by  $kT_C/8d$ , where  $k$  is Boltzmann's constant,  $T_C$  is the Curie temperature, and  $d$  is the nearest neighbor distance between spins in a direction normal to the domain wall. Both  $A$  and  $d$  have ambiguity for a structure such as that of  $\text{Co}_5\text{R}$  compounds, in which there are two moment-bearing elements and two nonequivalent sites for cobalt atoms. However, a logical choice for  $d$  appears to be  $a/2$ . Using these distances, we have included in Table II values of  $Ad/kT_C$ . The values vary, and differ significantly from 0.125. Although some of the variation may be associated with experimental error, we feel the discrepancies are large enough to indicate that this common approximation for  $A$  is somewhat inaccurate for these materials.

The standard continuum model of a domain wall also leads to the following equation for the thickness of a domain wall:<sup>(7)</sup>

$$\delta = \pi(A/K)^{1/2} = \pi\gamma/4K \quad (3)$$

We have included in Table II values of  $\delta$  calculated from measured values of  $\gamma$  and  $K$ . These values indicate that the domain walls in these compounds are so thin that the continuum model may not be a satisfactory approximation, and discrete models considering detailed atomic positions<sup>(21, 22)</sup> may be necessary.

Our measurements of  $\gamma$  have confirmed the suggestion of Westendorp<sup>(5)</sup> that the domain-wall energy of  $\text{Co}_5\text{Sm}$  is higher than that of most other  $\text{Co}_5\text{R}$  compounds. However, he estimated that it may be as much as five times as great, whereas it is only two or three times as great according to our results. His estimates were made from observations on small grains of unknown shape and thickness, and this may account for the quantitative difference in our results.

TABLE II

Some Fundamental Magnetic Properties of Co<sub>5</sub>R Compounds\*

Material	Domain-Wall Energy $\gamma$ (ergs/cm <sup>2</sup> )	Anisotropy Constant K <sup>(16)</sup> (ergs/cm <sup>3</sup> )	Exchange Constant A (ergs/cm)	Curie Point <sup>(3)</sup> T <sub>C</sub> (°K)	Interatomic <sup>(20)</sup> Distance d (Å)	Ad <sub>TC</sub> (kT <sub>C</sub> )	Domain-Wall Thickness $\delta$ (Å)	Single-Domain Particle Size D <sub>C</sub> (μ)
Co <sub>5</sub> Sm	85	13•10 <sup>7</sup>	3.5•10 <sup>-6</sup>	1000	2.50	0.63	51	1.6
Co <sub>5</sub> Y	35	5	1.5	920	2.47	0.29	55	0.68
Co <sub>5</sub> Ce	25	3	1.3	650	2.46	0.36	65	0.92
Co <sub>5</sub> Pr	40	9	1.1	890	2.51	0.22	35	0.61

\*The measurements of W(T) and Eq. (1) directly yield  $\gamma/M_s^2$ . From this and Eq. (4), D<sub>C</sub> is calculated. Values of M<sub>s</sub> from Ref. 3 are used to calculate  $\gamma$ . Values of K from Ref. 16 and Eqs. (2) and (3) are used to calculate A and  $\delta$ .

Westendorp also speculates that the higher domain-wall energy of Co<sub>5</sub>Sm may explain why high coercive forces are more easily obtained with ground powders of this compound than of the other compounds. This is possible, because theories based on domain wall nucleation or pinning are likely to predict a coercive force proportional to  $\gamma$ , as does the pinning model of Zijlstra.<sup>(4)</sup> However, the differences in coercive forces obtained with similar processing of the various compounds are much greater than the differences in wall energy we have measured. High coercive forces are also very easily obtained with ground powders of Co<sub>5</sub>Gd.<sup>(23, 24)</sup> Although this is undoubtedly related in some way to the low magnetization of Co<sub>5</sub>Gd, we suggest that the quantity of most direct relevance is the particle size for single-domain behavior. The diameter of a sphere below which a single-domain structure is of lower energy than a multidomain structure is approximately<sup>(19)</sup>

$$D_C = 1.4 \gamma / M_s^2. \quad (4)$$

We have included D<sub>C</sub> values in Table II. Using our estimated  $\gamma$  values from Table I, we also estimate D<sub>C</sub> to be 0.29μ, 0.80μ, and 5.1μ for Co<sub>5</sub>Nd, Co<sub>5</sub>La, and Co<sub>5</sub>Gd, respectively.

It is known, of course, that high coercive forces can be obtained with particles considerably larger than D<sub>C</sub>. Commercial sintered Co<sub>5</sub>Sm magnets contain grains averaging 5μ to 10μ in diameter and, in a thermally demagnetized state, contain several domains per grain.<sup>(25)</sup> However, it is likely that the fundamental domain behavior of a particle of diameter D scales with D/D<sub>C</sub> or, equivalently, with DM<sub>s</sub><sup>2</sup>/γ. [The fundamental domain behavior of thin plates, discussed above, scales with TM<sub>s</sub><sup>2</sup>/γ,<sup>(6)</sup> as is evident from the equations for T<sub>1</sub> and T<sub>2</sub>.] Therefore, it seems likely that the optimum properties of various Co<sub>5</sub>R and Co<sub>17</sub>R<sub>2</sub> compounds with smaller D<sub>C</sub> than that of Co<sub>5</sub>Sm would be achieved at smaller particle sizes than for Co<sub>5</sub>Sm. For example, 2μ to 4μ diameter for Co<sub>5</sub>Y is equivalent to 5μ to 10μ for Co<sub>5</sub>Sm. Difficulties,

however, will be expected from the greater mechanical strains and increased oxidation associated with finer particles. This may explain why it has been found much more difficult to produce high coercive forces with most of the compounds than with Co<sub>5</sub>Sm and Co<sub>5</sub>Gd, which have a large D<sub>C</sub>.

We note that the equilibrium surface domain width on bulk specimens, discussed earlier, also scales with  $\gamma/M_s^2$ . Specifically, the wavelength  $\lambda$  of domain corrugations for Co<sub>5</sub>Sm was 6μ, of the order of the grain size used in commercial magnets. Thus such measurements may be useful as a crude but easy means of estimating the relative particle refinement necessary to achieve high coercive forces in sintered magnets of various materials. We have recently applied this criterion to domain patterns observed on several Co<sub>17</sub>R<sub>2</sub>, (Co, Fe)<sub>17</sub>R<sub>2</sub>, and Co<sub>7</sub>R<sub>2</sub> compounds.<sup>(26)</sup>

Finally, we should recall that the coercive force in these compounds is controlled by the nucleation and/or pinning of domain walls, and therefore is sensitive not only to fundamental magnetic properties such as K,  $\gamma$ , M<sub>s</sub>, and D<sub>C</sub>, but also to detailed defects in the metallurgical structure, such as surface irregularities, precipitates, cracks, dislocations, etc. Some of the differences in properties attained with different materials may of course be associated with differences in metallurgical defects rather than with differences in fundamental magnetic properties.

## SUMMARY

1. We have studied domain patterns in single-crystal plates of Co<sub>5</sub>R compounds with the easy magnetic axis normal to the plate. As thickness is decreased, the surface domain structure of corrugations and spike domains disappears and simple maze patterns are produced.

2. The variation of internal domain width with thickness T changes from T<sup>2/3</sup> to T<sup>1/2</sup> at a thickness roughly equivalent to that predicted by theory.

3. From measurements of equilibrium domain width in the  $T^{1/2}$  region we have determined domain-wall energies for several compounds, and from surface domain observations on bulk specimens we have estimated it for several others.

4. These measured values of wall energy correlate qualitatively with anisotropy constants measured by Tatsumoto et al.

5. From wall energies and anisotropy constants we have calculated exchange constants and domain-wall thicknesses. Domain-walls are so thin in these compounds, however, that the standard continuum model for a domain-wall may not be adequate.

6. Our measurements have confirmed Westendorp's suggestion that the wall energy of  $\text{Co}_5\text{Sm}$  is larger than that of other  $\text{Co}_5\text{R}$  compounds, but our results differ quantitatively from his estimates.

7. We have calculated the critical single-domain particle size  $D_C$  for various  $\text{Co}_5\text{R}$  compounds. It is higher for  $\text{Co}_5\text{Sm}$  and  $\text{Co}_5\text{Gd}$  than for the other compounds, and we suggest that this may partly explain why high coercive forces are more easily obtained in  $\text{Co}_5\text{Sm}$  and  $\text{Co}_5\text{Gd}$  than in the other compounds.

8. We suggest that measurements of surface domain width on bulk samples may be useful to estimate  $D_C$  and the optimum particle size for commercial sintered magnets.

#### ACKNOWLEDGMENTS

We acknowledge with thanks helpful discussions with J. J. Becker, M. G. Benz, I. S. Jacobs, and D. L. Martin.

This work was supported by the Advanced Research Projects Agency, Department of Defense, and was monitored by the Air Force Materials Laboratory, MAYE, under Contract F33615-70-C-1626.

#### NOTE ADDED IN PROOF:

Two recent theoretical estimates of domain-wall energy for  $\text{Co}_5\text{Sm}$  are  $36 \text{ ergs/cm}^2$  (27) and  $154 \text{ ergs/cm}^2$ . (28) The large difference between these two estimates results mostly from the uncertainty in the approximate equations used to relate  $\gamma$  to  $T_C$ ,  $K$ , and other known parameters. Considering these uncertainties, the result that both theoretical estimates are within about a factor of two of our experimental value of  $85 \text{ ergs/cm}^2$  should be considered reasonable agreement.

#### REFERENCES

1. J. J. Becker, J. Appl. Phys. 41, 1055 (1970).
2. K. J. Strnat and A. E. Ray, Z. Metallk. 61, 461 (1970); K. Strnat, IEEE Trans. Mag. 6, 182 (1970).
3. D. L. Martin and M. G. Benz, Proc. 1971 Conf. on Magnetism and Magnetic Materials, A. I. P. Conf. Proc. No. 5, Part 2, 970 (1972).
4. H. Zijlstra, J. Appl. Phys. 41, 4881 (1970); J. Appl. Phys. 42, 1510 (1971).
5. F. F. Westendorp, J. Appl. Phys. 42, 5727 (1971).
6. J. Kaczer, IEEE Trans. Mag. 6, 442 (1970); Sov. Phys. JETP 19, 1204 (1964).
7. D. J. Craik, Contemp. Phys. 11, 65 (1970); D. J. Craik and R. S. Tebble, Ferromagnetism and Ferromagnetic Domains, J. Wiley and Sons, Inc., New York (1965).
8. M. Rosenberg, C. Tanasoiu, and V. Florescu, J. Appl. Phys. 37, 3826 (1966).
9. E. A. Nesbitt, H. J. Williams, J. H. Wernick, and R. C. Sherwood, J. Appl. Phys. 33, 1674 (1962).
10. R. A. McCurrie and G. P. Carswell, J. Mater. Sci. 5, 825 (1970); R. A. McCurrie, G. P. Carswell, and J. B. O'Neill, J. Mater. Sci. 6, 164 (1970).
11. K. Bachmann, A. Bischofberger, and F. Hofer, J. Mater. Sci. 6, 169 (1971); K. Bachmann and F. Hofer, Z. angew. Phys. 32, 41 (1971); K. Bachmann, IEEE Trans. Mag. 7, 647 (1971).
12. R. G. Wells and D. V. Ratnam, IEEE Trans. Mag. 7, 651 (1971).
13. A. F. Turner, J. R. Benford, and W. J. McLean, Economic Geology 40, 18 (1945).
14. C. Kittel, Phys. Rev. 70, 965 (1946).
15. A. Hubert, Phys. Stat. Sol. 24, 669 (1967).
16. E. Tatsumoto, T. Okamoto, H. Fujii, and C. Inoue, Suppl. J. Physique 32, C1-550 (1971).
17. R. Gemperle and A. Gemperle, Phys. Stat. Sol. 26, 207 (1968).

18. H. A. Alperin, O. Steinsvoll, G. Shirane, and R. Nathans, J. Appl. Phys. 37, 1052 (1966).
19. J. Smit and H. P. J. Wijn, Ferrites, John Wiley and Sons, Inc., New York (1959).
20. W. A. J. J. Velge and K. H. J. Buschow, J. Appl. Phys. 39, 1717 (1968).
21. T. Egami and C. D. Graham, Jr., J. Appl. Phys. 42, 1299 (1971).
22. J. J. van den Broek and H. Zijlstra, IEEE Trans. Mag. 7, 226 (1971).
23. W. M. Hubbard, E. Adams, and J. V. Gilfrich, J. Appl. Phys. 31, 368S (1960).
24. K. H. J. Buschow and A. S. van der Goot, J. Less Common Metals 17, 249 (1969).
25. J. D. Livingston, to be published.
26. J. D. Livingston, submitted to J. Mater. Sci.
27. M. G. Benz and D. L. Martin, J. Appl. Phys. to be published.
28. R. A. McCurrie and G. P. Carswell, Phil. Mag. 23, 333 (1971).

J. D. Livingston  
(Submitted to the Journal of Materials Science)

## INTRODUCTION

The excellent permanent magnet properties of  $\text{Co}_5\text{R}^*$  compounds<sup>(1-3)</sup> are based on a high, positive, uniaxial magnetocrystalline anisotropy. This "easy-axis" magnetic symmetry produces magnetic domain patterns<sup>(4-8)</sup> of a type well characterized by earlier work on other easy-axis materials.<sup>(9-12)</sup>

The Co-R alloy system contains  $\text{Co}_{17}\text{R}_2$  and  $\text{Co}_7\text{R}_2$  phases with crystal structures closely related to that of the  $\text{Co}_5\text{R}$  compounds.<sup>(13)</sup> The  $\text{Co}_{17}\text{R}_2$  phases, of potential interest as permanent magnet materials, are generally of easy-plane, rather than easy-axis, magnetic symmetry. However, Ray and Strnat<sup>(14)</sup> have recently reported that partial substitution of iron for cobalt in some cases transforms the symmetry to easy-axis. The  $\text{Co}_7\text{R}_2$  phases are not of direct interest as permanent magnet materials, but are of indirect interest because optimum  $\text{Co}_5\text{R}$  magnets are hyperstoichiometric and contain several percent of  $\text{Co}_7\text{R}_2$ .<sup>(3, 15)</sup>

We have studied magnetic symmetries in several  $\text{Co}_{17}\text{R}_2$ ,  $(\text{Co}, \text{Fe})_{17}\text{R}_2$ , and  $\text{Co}_7\text{R}_2$  phases by means of magnetic domain observations.

## EXPERIMENTAL

Compounds were arc-cast from high-purity materials and studied metallographically either in the as-cast condition or after annealing overnight about 100° to 200°C below their respective melting points. Domains were observed in polarized light on a Bausch and Lomb metallograph, using an elliptical compensator<sup>(16)</sup> to optimize the contrast.

## RESULTS

As shown earlier by Becker,<sup>(1)</sup> an as-cast sample of  $\text{Co}_{17}\text{Sm}_2$  contains classic easy-axis domain structures (Fig. 1). Magnetic domain walls in such materials lie nearly parallel to the magnetization direction. Therefore, in grains in which this easy-axis has a substantial component in the surface plane, the domain patterns are elongated in this direction. However, in grains with the easy-axis nearly normal to the surface, "rosette" patterns are seen, as in the grain at the right in Fig. 1. These patterns result from a surface refinement of the domain structure that occurs to reduce magnetostatic energy.<sup>(6, 9-12)</sup> Domain walls become corrugated in the surface region, domains are split by reverse "spike" domains, and the resulting rosette patterns

are sufficiently characteristic that their observation can be taken as evidence of easy-axis magnetic symmetry. For example, Fig. 2(a) shows domains in a casting of composition  $(\text{Co}_{0.75}\text{Fe}_{0.25})_{17}\text{Sm}_2$ . This confirms results of Ray and Strnat<sup>(14)</sup> that easy-axis symmetry is retained in this system.

In contrast, we were unable to detect any magnetic domain structures in as-cast or annealed samples of  $\text{Co}_{17}\text{Pr}_2$ ,  $\text{Co}_{17}\text{Y}_2$ , or  $\text{Co}_{17}\text{Nd}_2$ . An as-cast sample of  $\text{Co}_{17}\text{Ce}_2$  contained two phases and faint lamellar domains, but an annealed sample was single phase and showed no domains. These results are consistent with earlier results that these four compounds have easy-plane rather than easy-axis symmetry.<sup>(1, 2, 14)</sup> Presumably the magnetization in each domain can rotate freely in the easy plane and, to decrease magnetostatic energy, will lie parallel to the surface. The Kerr-effect contrast in Co-R compounds arises primarily from the component of magnetization normal to the surface, and thus domains are not seen in these easy-plane materials. Substitution of iron for cobalt in  $\text{Co}_{17}\text{Pr}_2$ ,  $\text{Co}_{17}\text{Y}_2$ , and  $\text{Co}_{17}\text{Ce}_2$  transforms the magnetic symmetry to easy-axis,<sup>(14)</sup> as confirmed by the domain patterns in Figs. 2(b), (c), and (d).

Mechanically polished surfaces of  $\text{Co}_{17}\text{Gd}_2$  reveal a fine and complex domain structure (Fig. 3). This structure appears to be related to surface strain introduced by polishing, an effect well known in soft magnetic materials.<sup>(17)</sup> If a strain-free surface is prepared by electropolishing in phosphoric acid, a fine but very faint rosette domain pattern can be seen. (On  $\text{Co}_{17}\text{Sm}_2$  and other compounds tested, domains on mechanically polished and electropolished surfaces appeared the same.) We conclude that  $\text{Co}_{17}\text{Gd}_2$  is of easy-axis symmetry, but probably has a rather low crystal anisotropy. If 30 percent of the cobalt is replaced by iron, coarser easy-axis patterns of much stronger contrast are seen [Fig. 2(e)].

Prior to this work, no information was available on the magnetic symmetry of  $\text{Co}_7\text{R}_2$  compounds. As seen in Fig. 4, easy-axis patterns are seen in annealed samples of  $\text{Co}_7\text{Sm}_2$ ,  $\text{Co}_7\text{Pr}_2$ ,  $\text{Co}_7\text{Y}_2$ , and  $\text{Co}_7\text{Nd}_2$ . Domains were similar in  $\text{Co}_7\text{La}_2$ , but optical contrast was very low. Patterns were also easy-axis in as-cast samples, but were more complex because grain structure was fine and complex.

An interesting special case is  $\text{Co}_7\text{Gd}_2$ . Because the Gd and Co moments are antiparallel, this compound has a very low net moment,<sup>(18)</sup> which leads us to expect very large domains.<sup>(9-12)</sup> The domain size was in fact found to be comparable to the grain size, and domains were most easily recognized by comparing the same area before and after moving the domains with a magnet (Fig. 5). Our

\*R = rare earth, La, or Y.

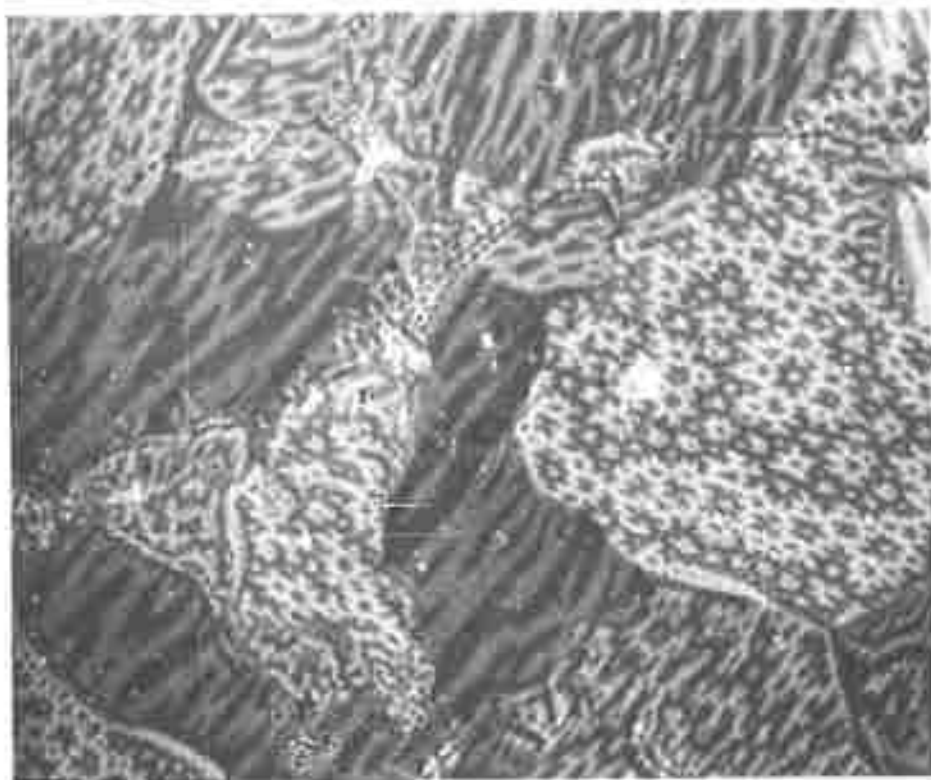
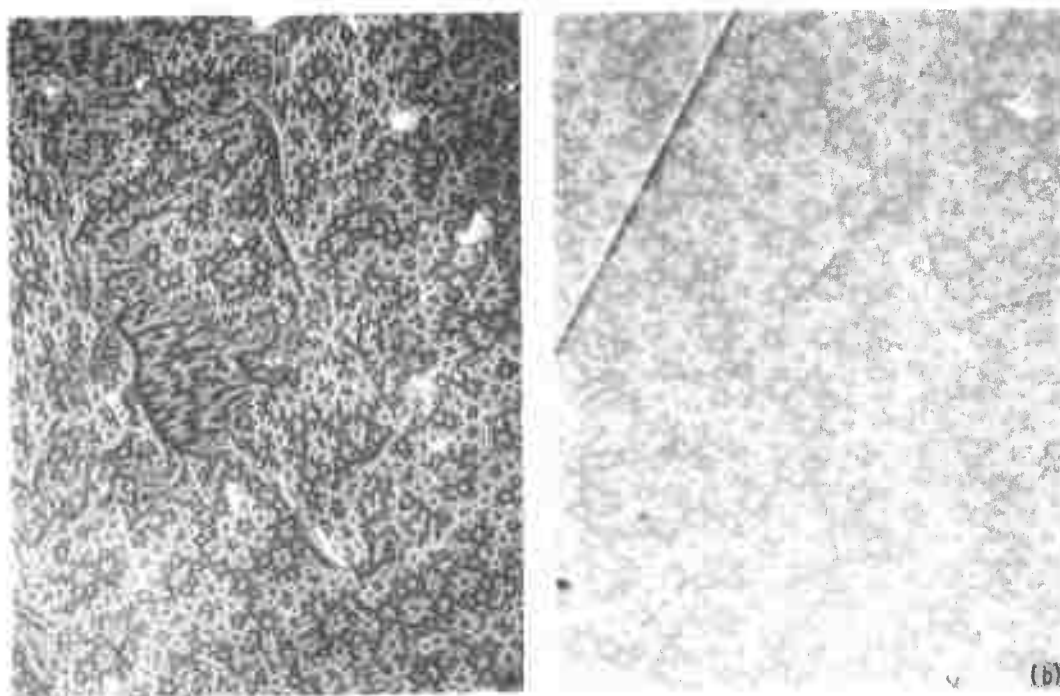


Fig. 1 Magnetic domains in  $\text{Co}_{17}\text{Sm}_2$ . Rosette structure in grain at right is characteristic of easy-axis magnetic symmetry (photograph from J. J. Becker). 530X



15

Fig. 2 Easy-axis domain patterns in (a)  $(\text{Co}_{0.75}\text{Fe}_{0.25})_{17}\text{Sm}_2$ , (b)  $(\text{Co}_{0.6}\text{Fe}_{0.4})_{17}\text{Pr}_2$ .

550X

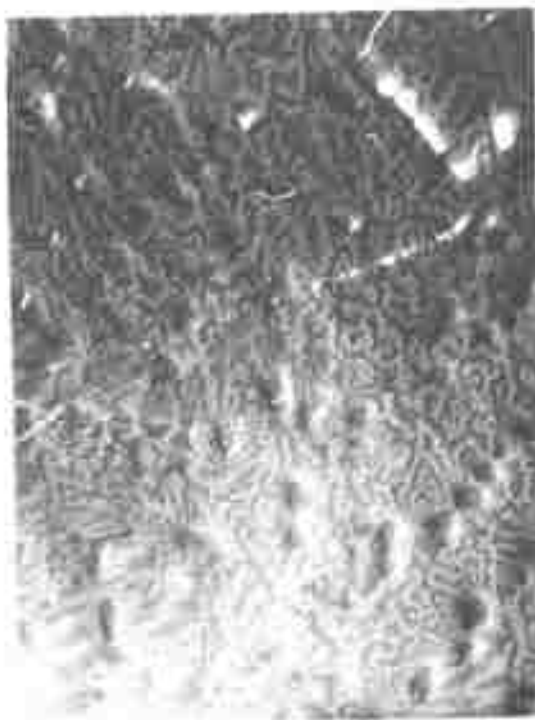


Fig. 2 (Contd) (c)  $(\text{Co}_{0.7}\text{Fe}_{0.3})_{17}\text{Y}_2$ , (a')  $(\text{Co}_{0.75}\text{Fe}_{0.25})_{17}\text{Ce}_2$ .

570X

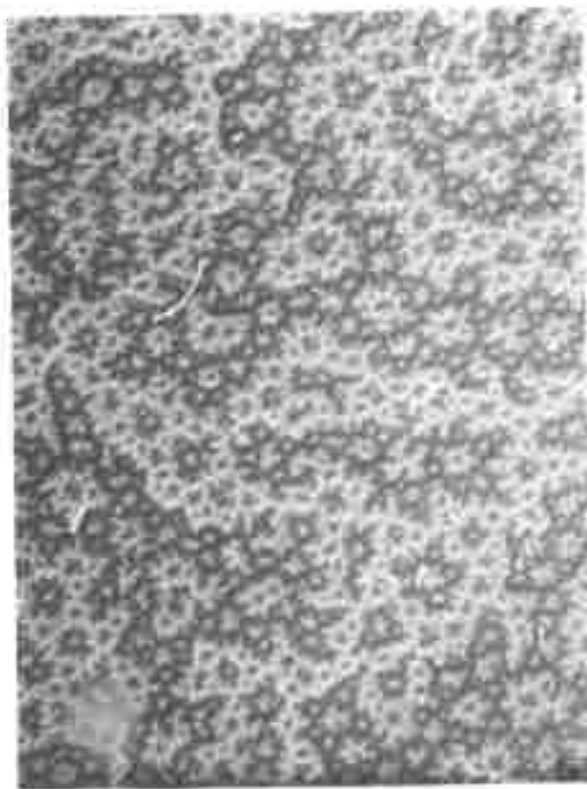


Fig. 2 (Concluded) (e)  $(\text{Co}_{0.7}\text{Fe}_{0.3})\text{Gd}_2$ . 620X

observations on this sample were consistent with earlier observations on easy-axis materials with low moment.<sup>(9-12)</sup>

#### SUMMARY AND DISCUSSION

Characteristic easy-axis domain patterns were seen in  $\text{Co}_{17}\text{Sm}_2$ ,  $\text{Co}_{17}\text{Gd}_2$ , and several  $(\text{Co}, \text{Fe})_{17}\text{R}_2$  and  $\text{Co}_7\text{R}_2$  compounds. Domains were not seen in  $\text{Co}_{17}\text{Pr}_2$ ,  $\text{Co}_{17}\text{Y}_2$ ,  $\text{Co}_{17}\text{Nd}_2$ , or  $\text{Co}_{17}\text{Ce}_2$ .

In a recent study of domain widths and domain-wall energies in  $\text{Co}_5\text{R}$  compounds,<sup>(19)</sup> it was suggested that the wavelength of surface domain corrugations on bulk samples may be a rough measure of the fineness of grain size necessary to produce good coercive forces in sintered magnets. For example, this dimension was about  $6\mu$  in  $\text{Co}_5\text{Sm}$ ,  $3\mu$  in  $\text{Co}_5\text{Pr}$ , and  $30\mu$  in  $\text{Co}_5\text{Gd}$ . Applying this criterion to the domain patterns reported above, we estimate this dimension to be  $1\mu$  to  $2\mu$  in  $\text{Co}_{17}\text{Gd}_2$  and the various  $(\text{Co}, \text{Fe})_{17}\text{R}_2$  compounds,  $2\mu$  to  $3\mu$  for  $\text{Co}_{17}\text{Sm}_2$  and most of the  $\text{Co}_7\text{R}_2$  compounds,  $5\mu$  for  $\text{Co}_7\text{Sm}_2$ , and very large but undetermined for  $\text{Co}_7\text{Gd}_2$ . In combination with saturation magnetization values, these dimensions may also be used to estimate domain-wall energies.<sup>(19)</sup>

#### ACKNOWLEDGMENTS

We are grateful to J. J. Becker for allowing us to use Fig. 1 and for providing many of the samples. Metallography was done by M. B. McConnell,

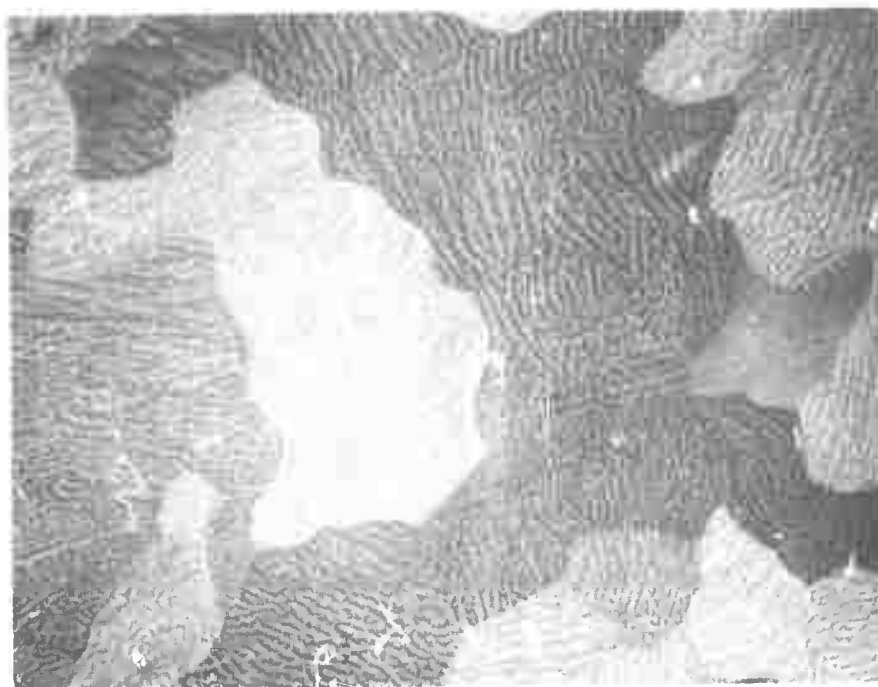
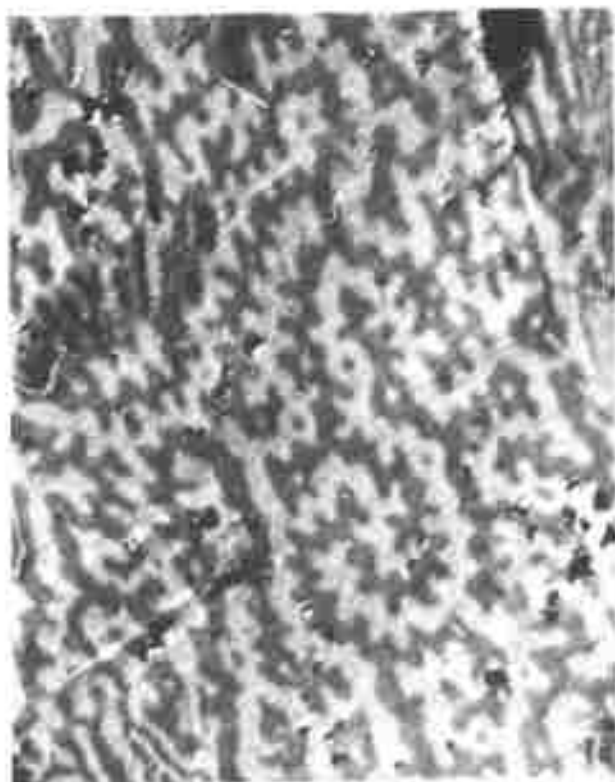


Fig. 3 Domain patterns in mechanically polished  $\text{Co}_{17}\text{Gd}_2$ . These maze patterns are believed to be caused by surface strains. 690X



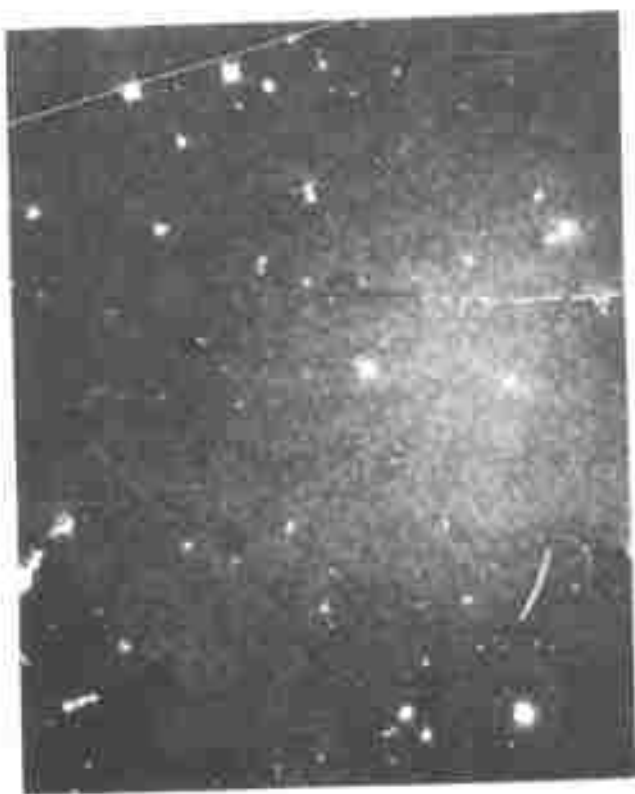


Fig. 4 (Concluded) Easy-axis domain patterns in (c)  $\text{Co}_7\text{Y}_2$ , and (d)  $\text{Co}_7\text{Nd}_2$ .

676X

D. Marsh, and A. Ritzer. This work was supported by the Advanced Research Projects Agency, Department of Defense, and was monitored by the Air Force Materials Laboratory, MAYE, under Contract F33615-70-C-1626.

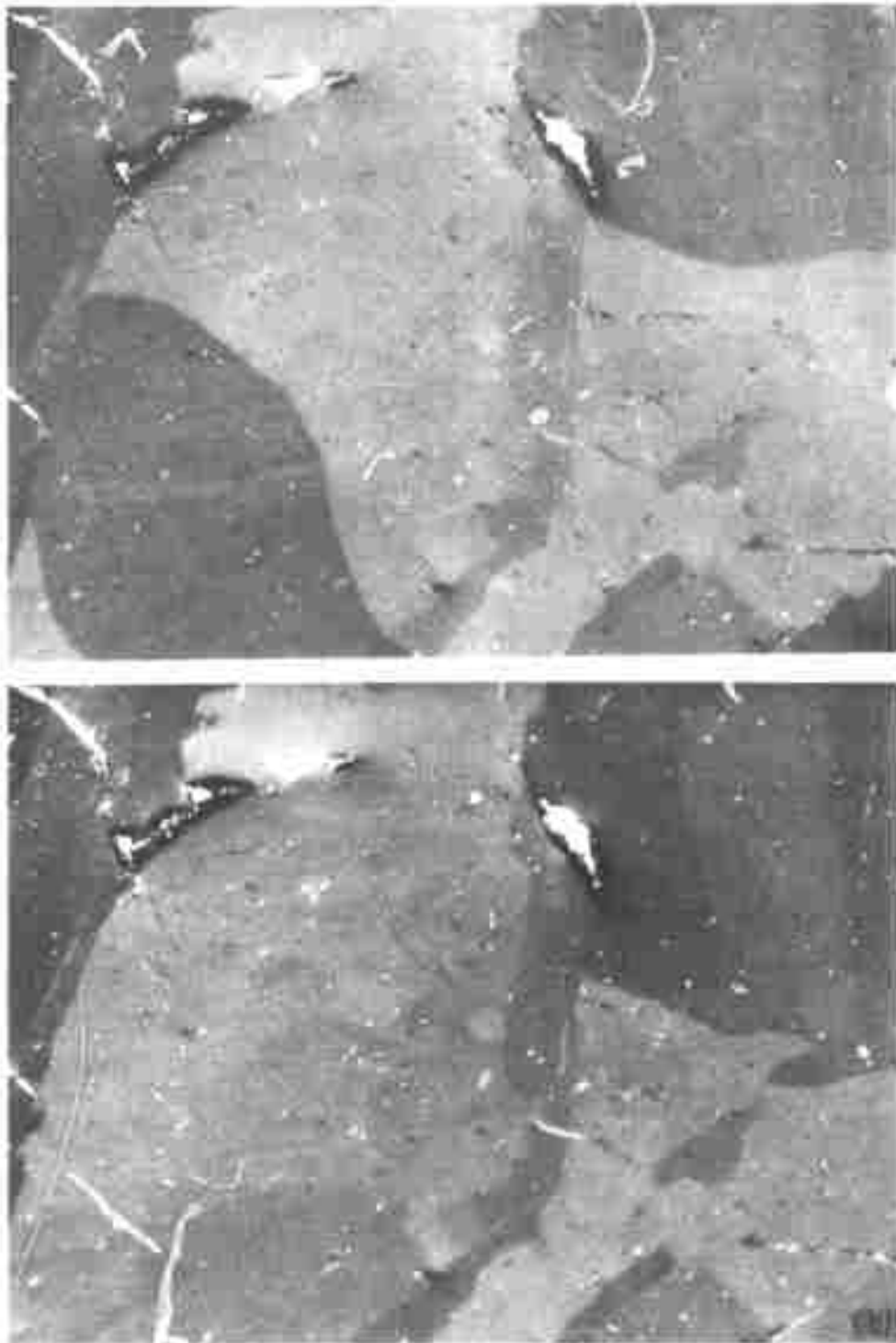


Fig. 5 Magnetic domains in  $\text{Co}_7\text{Gd}_2$  (a) before and (b) after touching sample with a magnet. Note downward motion of domain wall at right center and disappearance of dark domain at lower left. Domains are large because of low magnetic moment. 469X

## REFERENCES

1. J. J. Becker, J. Appl. Phys. 41, 1055 (1970).
2. K. J. Strnat and A. E. Ray, Z. Metallk. 61, 461 (1970); K. Strnat, IEEE Trans. Mag. 6, 182 (1970).
3. D. L. Martin and M. G. Benz, Proc. 1971 Conf. on Magnetism and Magnetic Materials, Am. Inst. Physics Conf. Proc. No. 5, p. 970 (1972).
4. E. A. Nesbitt, H. J. Williams, J. H. Wernick, and R. C. Sherwood, J. Appl. Phys. 33, 1674 (1962).
5. R. A. McCurrie and G. P. Carswell, J. Mater. Sci. 5, 825 (1970); R. A. McCurrie, G. P. Carswell, and J. B. O'Neill, J. Mater. Sci. 6, 164 (1970).
6. K. Bachmann, A. Bischofberger, and F. Hofer, J. Mater. Sci. 6, 169 (1971); K. Bachmann and F. Hofer, Z. Angew. Physik 32, 41 (1971); K. Bachmann, IEEE Trans. Mag. 7, 647 (1971).
7. R. G. Wells and D. V. Ratnam, IEEE Trans. Mag. 7, 651 (1971).
8. F. F. Westendorp, J. Appl. Phys. 42, 5727 (1971).
9. J. Kaczer, IEEE Trans. Mag. 6, 442 (1970); Soviet Phys. -JETP 19, 1204 (1964).
10. M. Rosenberg, C. Tanasoiu, and V. Florescu, J. Appl. Phys. 37, 3826 (1966).
11. A. Hubert, Phys. Stat. Sol. 24, 669 (1967).
12. D. J. Craik, Contemp. Phys. 11, 65 (1970); D. J. Craik and R. S. Tebble, Ferromagnetism and Ferromagnetic Domains, John Wiley and Sons, Inc., New York (1965).
13. K. H. J. Buschow, Phys. Stat. Sol. (a) 7, 199 (1971); Philips Res. Repts. 26, 49 (1971).
14. A. E. Ray and K. J. Strnat, 1972 Intermag. Conf., Kyoto, to be published in IEEE Trans. Mag. 8 (1972).
15. R. L. Cech, J. Appl. Phys. 41, 5247 (1970); D. K. Das, IEEE Trans. Mag. 7, 432 (1971).
16. A. F. Turner, J. R. Benford, and W. J. McLean, Economic Geol. 40, 18 (1945).
17. S. Chikazumi and K. Suzuki, J. Phys. Soc. Japan 10, 523 (1955).
18. R. Lemaire, Cobalt 33, 201 (1966).
19. J. D. Livingston, submitted to J. Appl. Phys.

### III. MATERIALS CHARACTERIZATION AND PHASE EQUILIBRIUM STUDIES

#### 1. Summary of analytical results by wet chemistry and x-ray fluorescence spectroscopy (J. G. Smeggil)

It is becoming increasingly evident that the magnetic properties of cobalt-rare-earths are closely related to their chemical composition. Nevertheless, quantitative analytical chemical procedures are little used in characterizing these materials. Standard analytical practices are time-consuming and of questionable reliability.

The objective of this work was to establish a fast, accurate instrumental technique for these materials which could establish all major constituents to  $\pm 0.10$  wt % within an hour. The technique of x-ray fluorescence analysis was selected for application toward this goal.

Before proceeding with the development of any instrumental technique, it is necessary to prepare suitable samples for composition standards, established by classical analytical methods.

Two different laboratories analyzed a series of specimens, using somewhat different techniques. The results are summarized in Fig. 1. They indicate very good agreement in the variation from one sample to another, but an absolute difference of approximately 0.5 wt %. While the origin of this difference has not yet been traced to the analytical procedures, the samples are entirely usable as self-consistent composition standards based on either one of the sets of reported values. They have been used in this way to evaluate x-ray fluorescence spectroscopy procedures.

A number of different instrumental techniques were considered, including atomic absorption, solution spectrophotometry, emission spectroscopy, and x-ray fluorescence. For various reasons only the last was considered worthy of further evaluation.

Results from two outside laboratories gave virtually random scatter in counting rate as a function of composition over a range of about 4 wt %. It was then decided to optimize the procedure using the equipment available at the General Electric Research and Development Center.

A very thorough study of counting time, sample configuration, recording method, linearity, noise, 2 $\theta$  optimization, stability, and other parameters was made. Data taken on two different days on four samples, along with an "unknown" sample, are summarized in Fig. 2. It is felt that the precision of these results is limited by the particular instrument used, and that with currently available equipment the objectives of this program would be fully realized.

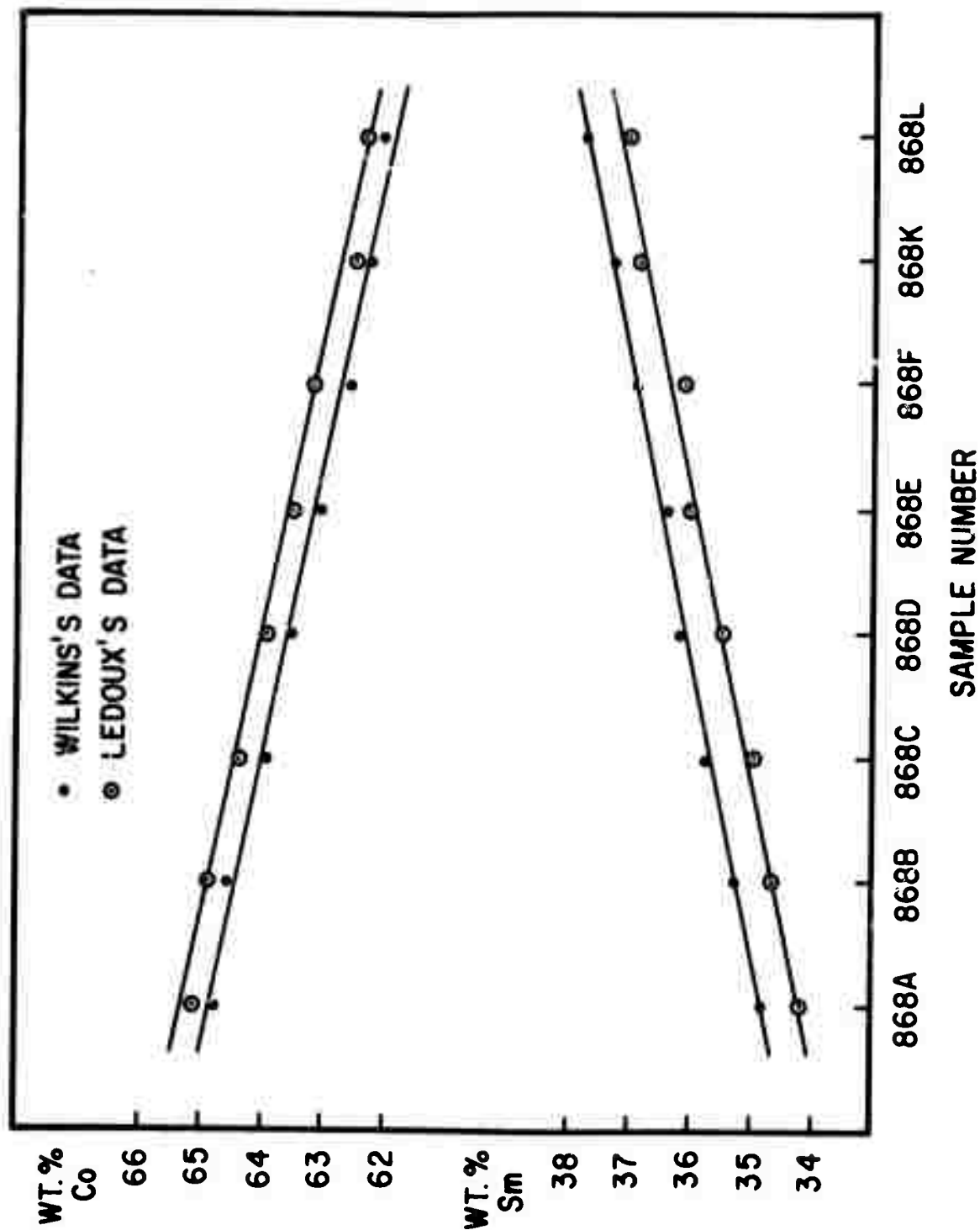


Figure 1 Comparison of analytical data from two sources on series of Co-Sm alloys.

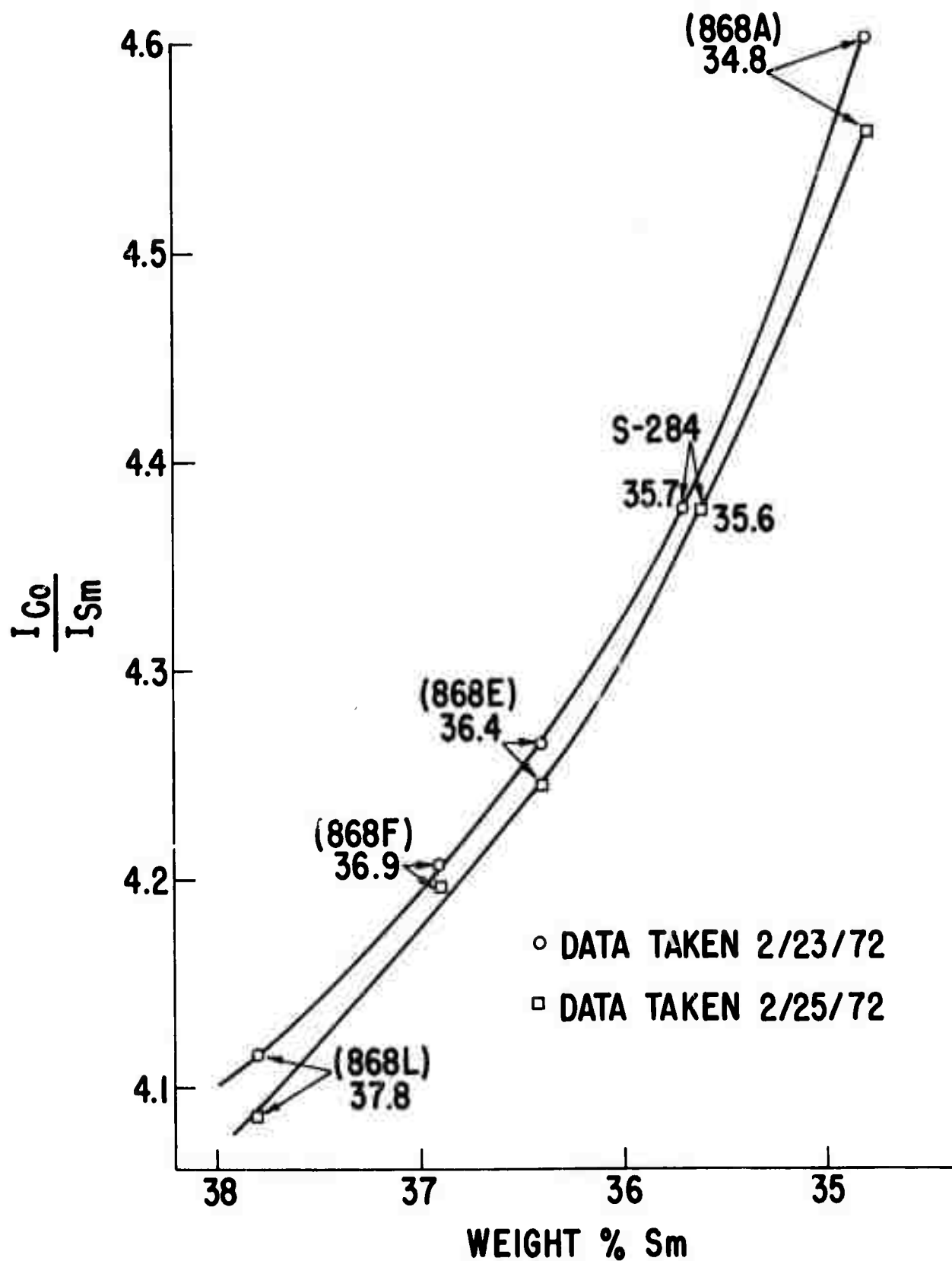


Figure 2 X-ray fluorescence intensity ratio data taken on four samples on two different days.

S. Foner, \* E. J. McNiff, Jr., \* D. L. Martin, † and M. G. Benz†  
(Applied Physics Letters, Vol. 20, No. 11, 1 June 1972, p. 447)

High energy-product permanent magnet materials have been developed with rare earth-cobalt alloys (Refs. 1-6), particularly with Sm-Co. In this report we describe properties of a Sm-Co alloy with an energy-product of 24 MGOe, the largest reported to date for this material. By optimizing parameters of fabrication, nearly complete alignment of the magnetic particles was achieved with a relative density which is 95% of the theoretical maximum (calculated from x-ray data). Because of the exceptional alignment, saturation of the magnetic moment could be achieved in this highly anisotropic material at an applied field well below the maximum of 140 kOe used for these experiments. Thus, in addition to the large energy-product, we observe a saturation moment  $\sim 10\%$  or more above that reported in earlier literature. (7-13)

The sample was prepared by a liquid-phase sintering process which has been used successfully to make high-energy cobalt-samarium permanent magnets. (4-5) A  $\text{Co}_5\text{Sm}$  base metal powder and a 60 wt % Sm - 40 wt % Co additive powder were blended to a nominal composition of 36 wt % Sm. The blended powder was made into a test bar by aligning the powder in a rubber tube in a 60 kOe magnetic field. The aligned powder was compressed slightly while still in the field to stabilize the particle alignment. Subsequently the bar was hydropressed at 200 kpsi to a relative density of about 80%. The bar was ground into a cylinder, and sintered in an argon atmosphere at 1135°C for 1 hour.

The sample was given a post-sintering treatment of 20 minutes at 1100°C, slow cooled to 850°C, held for 1 hour at that temperature, and cooled rapidly to room temperature.

The sample had a relative density of 94.6% of 8.6 g/cm<sup>3</sup>, and was 0.256 inch (0.65 cm) diameter by 1.06 inches (2.69 cm) long. Magnetic measurements at fields up to 60 kOe were made on the sintered bar prior to cutting it into shorter pieces for x-ray lattice parameter measurements, oxygen determination, and additional magnetic measurements at higher fields.

\*Francis Bitter National Magnet Laboratory, Massachusetts Institute of Technology, Cambridge, Mass. 02139. (Supported by U. S. Air Force and The National Science Foundation.)

†The research carried out at GE Corporate Research and Development, Schenectady, N. Y. 12301 was supported by the Advanced Research Projects Agency of the Department of Defense and was monitored by the Air Force Materials Laboratory, MAYE, under Contract F33615-70-C-1626.

During the processing the oxygen content of the alloy increased. In the sintered sample the oxygen was determined by vacuum fusion analysis to be  $0.46 \pm 0.2$  wt %. Assuming all the oxygen reacts with some of the Sm to form  $\text{Sm}_2\text{O}_3$ , the composition of the magnet material, based on chemical analyses, was 63.7 wt % Co, 32.6 wt % Sm, and 3.3 wt %  $\text{Sm}_2\text{O}_3$ . The sample also contains 0.26 wt % Ni and 0.07 wt % Al. The Sm content of the metallic phase is calculated to be 16.7 at. %.

The hexagonal lattice constants for the  $\text{Co}_5\text{Sm}$  phase measured on powder from the sintered bar were:  $a = 5.002 \pm 0.002 \text{ \AA}$ ,  $c = 3.963 \text{ \AA} \pm 0.001 \text{ \AA}$ , and cell volume =  $85.94 \text{ \AA}^3$ . The calculated density of the  $\text{Co}_5\text{Sm}$  phase was 8.60 g/cm<sup>3</sup>.

Magnetic measurements were made on the heat-treated bar by ballistic methods<sup>(14)</sup> in a superconducting solenoid with a peak field of 60 kOe, and on a disk cut from the center of the same bar, in water-cooled Bitter solenoids with a maximum field of 140 kOe.

Since the sample contains an appreciable volume of voids and  $\text{Sm}_2\text{O}_3$ , we report the saturation value for the ideal magnetic Co-Sm alloy as well as the measured values for the sample. The saturation moment per unit mass of the alloy,  $\sigma_s(\text{alloy})$ , is related to the saturation moment per unit mass of the sample,  $\sigma_s$ , by the following:

$$\sigma_s(\text{alloy}) = \sigma_s / X_w, \quad (1)$$

where  $X_w$  is the weight fraction of the alloy in the sample (0.978 for the sample used in this study). Similarly, the magnetization or magnetic moment per unit volume of the alloy,  $4\pi J_s(\text{alloy})$  is related to that the sample,  $4\pi J_s$ , by the relation:

$$4\pi J_s(\text{alloy}) = 4\pi J_s / X_v, \quad (2)$$

where  $X_v$  is the volume fraction of the alloy in the sample (0.929 for sample studied). The volume fraction is related to the weight fraction by the relation:

$$X_v = \frac{\rho(\text{sample})}{\rho(\text{alloy})} X_w. \quad (3)$$

The magnetic moment measurements on the thin disk were made with a low-frequency vibrating sample magnetometer.<sup>(15)</sup> The field was furnished by water-cooled Bitter solenoids with a maximum

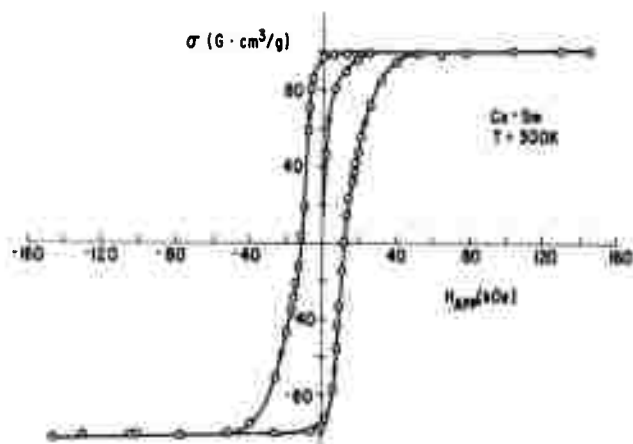


Fig. 1 Magnetic moment,  $\sigma$ , vs applied field  $H_{APP}$  for a small disk of Co-Sm magnet. The high degree of alignment is evidenced by saturation above 80 kOe.

TABLE I

Properties of a 63.7 Wt % Co, 32.6 Wt % Sm, 3.3 Wt %  $Sm_2O_3$   
Magnet Material as a Function of Temperature

Temperature (°K)	300	300	77	4.2
Magnetizing field (kOe)	60	100	100	100
Sample length/diameter	4.12	0.635	0.635	0.635
Demagnetizing factor	$\sim 0.027^{(a)}$	$\sim 0.4^{(b)}$	$\sim 0.4^{(b)}$	$\sim 0.4^{(b)}$
Density $\rho$ (sample)(g/cm³)	8.17	8.17	8.17	8.17
Density $\rho$ (alloy)(g/cm³)	8.6	8.6	8.6	8.6
Weight fraction (alloy), $X_w$	0.967	0.967	0.967	0.967
Volume fraction (alloy), $X_v$	0.918	0.918	0.918	0.918
$\sigma_s$ (G-cm³/g)	97.4	98.4	102.5	103.0
$\sigma_s$ (alloy)(G-cm³/g)	100.7	101.8	106.0	106.5
$4\pi J_s$ (kG)	10.0	10.1	10.5	10.6
$4\pi J_s$ (alloy)(kG)	10.9	11.0	11.4	11.5
$\sigma_r$ (G-cm³/g)	95	95.5	101	102
$4\pi J_r$ (kG)	9.7	9.8	10.4	10.5
$H_c$ (kOe)	-9.5	-8.7	-10.3	-10.1
$H_k$ (kOe)	-10.0	-8.5±1	-14.7±1	-16.3±1
$H_{ci}$ (kOe)	-13.2	-12	-19.0	-20.6
$(BH)_{max}$ (MGOe)	23.4	24.0±0.5	28±1	27±1
Alignment factor A	0.97	0.97	0.98	0.99

Notes for Table I:

(a) - Ballistic demagnetization factor,  $N_b$  (Ref. 16).

(b) - Magnetometric demagnetization factor,  $N_m$  (Ref. 16).

$\sigma_s$  - Saturation moment per unit mass of sample.  $\sigma_s \approx \sigma$  measured at  $H_m$ .

$\sigma_s$ (alloy) - Saturation moment per unit mass of the Co-Sm alloy in the sample  $\sigma_s$ (alloy) =  $\sigma_s/X_w$ .

$4\pi J_s$  - Saturation moment per unit of sample volume  $4\pi J_s = 4\pi\sigma_s\rho$ (sample).

$4\pi J_s$ (alloy) - Saturation moment per unit of alloy volume in the sample.

$$4\pi J_s(\text{alloy}) = 4\pi\sigma(\text{alloy})\rho(\text{alloy}) = 4\pi J_s/X_v$$

$\sigma_r$  - Remanent moment per unit of sample mass at  $H = 0$ .

$4\pi J_r$  - Magnetic moment per unit of sample volume at  $H = 0$ .  $4\pi J_r = 4\pi\sigma_r\rho$ (sample)

A - Alignment factor =  $\sigma_r/\sigma_s = 4\pi J_r/4\pi J_s$ .

$H_k$  - Demagnetizing field for which  $4\pi J = (0.9)4\pi J_r$ .

$H_c$  - Demagnetizing field for  $B = 0$ .

$H_{ci}$  - Demagnetizing field for  $4\pi J = 0$ .

field of 140 kOe. The sample and detection coils were surrounded by suitable Dewars in order to maintain constant temperatures and measurements were made at 300°, 77°, and 4.2°K. The accuracy of the magnetic moment measurements is well within 2% and the applied field is known to at least 1%.

The magnetic moment per unit mass  $\sigma$  vs the applied field  $H_{APP}$  is shown in Fig. 1 for the Co-Sm alloy at room temperature. (We will present measured quantities throughout the text and tabulate derived quantities when indicated.) The sample is a right circular cylinder with its axis parallel to  $H_{APP}$ . The dimensions of the sample were 0.192 inch in diameter and 0.122 inch in length. Several features are noteworthy: (1) saturation is achieved for an applied field of about 80 kOe; and (2) above this field,  $\sigma$  is almost constant--the susceptibility  $\Delta\sigma/\Delta H_{APP}$  is less than  $2 \times 10^{-5}$  G-cm<sup>3</sup>/g-Oe above saturation for  $4.2 \leq T \leq 300$  K. Assuming that this small effect may be due to misaligned crystallites we estimate that less than 2% of the material is misaligned (assuming an anisotropy field of  $\approx 250$  kOe); (3) the value of  $\sigma = \sigma_s$  at 300 K is 10% larger than that reported recently for single-crystal Co<sub>5</sub>Sm;<sup>(12)</sup> and also higher than reported on aligned powder or sintered samples. (5, 7-13)

The general features of Fig. 1 are maintained as the temperature is reduced; the area of the hysteresis loop increases somewhat and the value of  $\sigma_s$  increases slightly. Several properties of this Co<sub>5</sub>Sm material are tabulated in Table I. The values of  $\sigma_s$  at each temperature are larger than reported earlier<sup>(8, 12)</sup> and the temperature dependence of  $\sigma_s$  is somewhat smaller than reported earlier. (8, 12) The reasons for these differences are not clear. However, one possible source of error in the earlier data may be that the measurements were made at fields below that needed for saturation. A second possibility may involve differences in alloy composition or the presence of substantial amounts of oxide.

To correct the data in Fig. 1 to the conventional B-H plots we require a measure of the demagnetization or depolarizing factor as well as the actual density of the material. Measurements of the density yields  $\rho = 8.17$  g/cm<sup>3</sup>; close to the x-ray density  $\rho(\text{alloy}) = 8.6$  g/cm<sup>3</sup>. Estimates of the depolarizing factor were obtained from Joseph's tabulation<sup>(16)</sup> from which we obtain  $N_m = 0.4$ . Using these data, the derived quantities involving the magnetization (per unit volume) were calculated. These quantities are tabulated in Table I along with the maximum energy-products obtained from B versus H plots. The results for 77° and 4.2°K are included for comparison. It is apparent that a small variation in the  $(BH)_{max}$  occurs as a function of temperature. Because  $N_m$  is not exactly known for our geometry, the values of  $N_m$  were varied from 0.35 to 0.45, but essentially no change in the calculated  $(BH)_{max}$  was observed.

Other quantities in Table I include A (the alignment factor =  $\sigma_r/\sigma_s$ ), the alloy saturation moment,

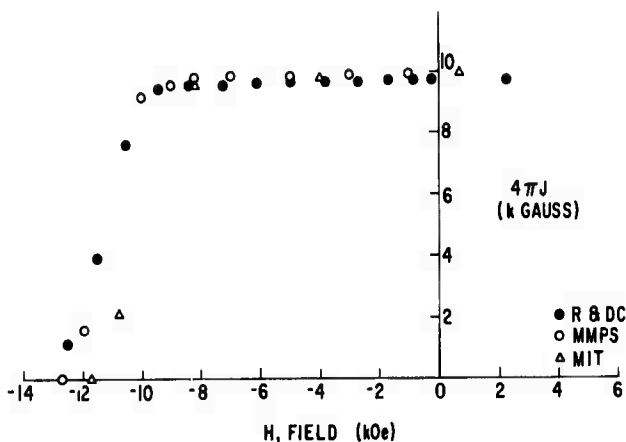


Fig. 2 Comparison of test results obtained on a long sintered bar as measured at the GE Magnetic Materials Product Section, Edmore, Mich., and CR&D with results measured on a disk at MIT.

and  $H_k$  which gives a measure of the shape of the hysteresis loop. Data for the long sintered bar at 300 K are also listed for comparison with the thin disk results, and plotted in Fig. 2 together with test results measured on the sintered bar at the General Electric Magnetic Materials Product Section, Edmore, Mich. The agreement is good considering that the bar was only magnetized at 60 kOe. The differences in the coercive force measurements are within experimental error.

The appreciable increase in  $(BH)_{max}$  over previous Co<sub>5</sub>Sm permanent magnet materials<sup>(1-5)</sup> is clearly due to the very nearly complete alignment of the compacted small magnetic particles together with a high relative density. This increase also is reflected in the larger value of  $\sigma_s(\text{alloy})$  which is a basic property of the compound. Based on these results it is expected that appreciable gains in  $(BH)_{max}$  and  $\sigma_s$  will be realized when other Co rare-earth permanent magnet materials are fabricated under optimum conditions for complete alignment. Such experiments are now in progress.

#### ACKNOWLEDGMENTS

We wish to thank J. Geertsens, W. Moore, and A. C. Rockwood of General Electric Corporate Research and Development for their help in the preparation, heat treatment, and ballistic testing of the Co-Sm sample.

We thank R. J. Parker of the Magnetic Materials Product Section, Edmore, for providing magnetic test results on the sintered bar for use in Fig. 2.

## REFERENCES

1. K. H. J. Buschow, W. Luiten, P. A. Naastepad, and F. F. Westendorp, *Philips Tech. Rev.* 29, 336 (1968).
2. K. H. J. Buschow, W. Luiten, and F. F. Westendorp, *J. Appl. Phys.* 40, 1309 (1969).
3. D. K. Das, *IEEE Trans. Magnetics* MAG-5, 214 (1969).
4. M. G. Benz and D. L. Martin, *Appl. Phys. Letters* 17, 176 (1970).
5. D. L. Martin and M. G. Benz, *Cobalt*, No. 50, 11 (1971).
6. J. Tsui and K. Strnat, *Appl. Phys. Letters* 18, 107 (1971).
7. K. Nassau, L. V. Cherry, and W. E. Wallace, *J. Phys. Chem. Solids* 16, 123 (1960).
8. E. A. Nesbitt, H. J. Williams, J. H. Wernick, and R. C. Sherwood, *J. Appl. Phys.* 32, 342S (1961).
9. K. Strnat, G. Hoffer, J. Olson, W. Ostertag, and J. J. Becker, *J. Appl. Phys.* 38, 1001 (1967).
10. W. A. J. J. Velge and K. H. J. Buschow, *J. Appl. Phys.* 39, 1717 (1968); also *Z. angew. Phys.* 26, 157 (1969).
11. K. H. J. Buschow, W. Luiten, and F. F. Westendorp, *J. Appl. Phys.* 40, 1309 (1969).
12. E. Tatsumoto, T. Okamoto, H. Fujii, and C. Inoue, *J. Physique* 32, C1-550 (1971).
13. H. Umebayashi and Y. Fujimura, *Japan. J. Appl. Phys.* 10, 1585 (1971).
14. M. G. Benz and D. L. Martin, *IEEE Trans. Magnetics* MAG-7, 285 (1971).
15. S. Foner and E. J. McNiff, Jr., *Rev. Sci. Instr.* 39, 171 (1968).
16. R. I. Joseph, *J. Appl. Phys.* 37, 4639 (1966).

# TEMPERATURE VARIATION OF COERCIVITY FOR Co-Sm PERMANENT MAGNET ALLOYS\*

D. L. Martin and M. G. Benz

(1972 Intermag Conference. Submitted to IEEE Transactions on Magnetics)

## INTRODUCTION

Changes in the magnetic properties of  $\text{Co}_5\text{R}$  permanent magnet alloys with temperature are of interest for two reasons:

1. The usefulness of a particular alloy will depend upon how much the magnetization of that alloy changes with temperature over the operating range of the device.

2. An understanding of how and why the changes in magnetization occur with changes in temperature might contribute to our overall understanding of the basic factors which govern coercivity. This property currently limits the performance of many  $\text{Co}_5\text{R}$  alloys.

A strong temperature dependence of intrinsic coercivity has been noted for  $\text{Co}_5\text{La}$ <sup>(1, 2)</sup> and  $\text{Co}_5\text{Sm}$  (Refs. 2, 3) powder samples. The intrinsic coercive force,  $H_{ci}$ , for each alloy was observed to increase by a factor of two as the temperature decreased from 300° to 80°K. This change of coercivity with temperature continues with increasing temperatures above room temperature, decreasing as the temperature increases, and relates to the irreversible losses which occur when Co-Sm magnets are heated.<sup>(4)</sup>

Westendorp<sup>(5)</sup> has explained the increase of coercivity with decreasing temperature on the basis of an increase of domain-wall energy with decreasing temperature. He cited an increase of domain spacing by a factor of 1.5 between 300° and 90°K to explain the factor of two increase of coercive force over the same temperature range.

McCurrie<sup>(3)</sup> and Gaunt<sup>(6)</sup> have proposed that the observed temperature effect can be accounted for by a thermal activation process in which magnetization reversal is assisted by thermal energy. The simple model proposed is domain wall pinning by inhomogeneities.<sup>(6)</sup>

In this report we describe a study in which the magnetic measurements on sintered magnets have been extended to cover a wider temperature range 4.2° to 750°K, and have included samples with a wide variation of coercivity values due to variations in composition and processing.

## EXPERIMENTAL

The sintered test bars were about 0.75 cm in diameter by 2.5 cm long. The magnetization was measured by a point-by-point ballistic method described previously.<sup>(7)</sup> The applied field was provided by either a 5 kOe copper solenoid or a 100 kOe superconducting solenoid. The sample and pickup coils were surrounded by suitable dewars. Below 80°K, measurements were made at the boiling points of helium, neon, and nitrogen. Between 80° and 300°K the system was first cooled with liquid nitrogen, and measurements were made as the sample heated slowly. Above 300°K the sample was heated by a small electric furnace. Sufficient data were obtained to plot the demagnetization curves at all the test temperatures, except above 500°K where only the  $H_{ci}$  value was determined. The usual procedure was to magnetize the sample in a 60 kOe field at room temperature before heating or cooling to the test temperature.

## RESULTS

In Fig. 1 the demagnetization vs temperature results are plotted for a sintered Co-Sm magnet with the following room-temperature properties:  $4\pi J$  (at 60 kOe) = 10 kG,  $B_r$  = 9.4 kG,  $H_c$  = -9.2 kOe,  $H_{ci}$  = -20 kOe, and  $(BH)_{\max}$  = 21.4 MGOe. The remanent magnetization  $4\pi J_r$  and intrinsic coercive force  $H_{ci}$  increase significantly with decreasing temperature, except at very low temperatures. At 4.2°K the  $H_{ci}$  value was slightly lower than that measured at 27.1°K. After testing at high or low temperatures the properties at room temperature were recoverable by remagnetization.

A summary of the test results for a series of sintered magnets is presented in Fig. 2. The coercivity

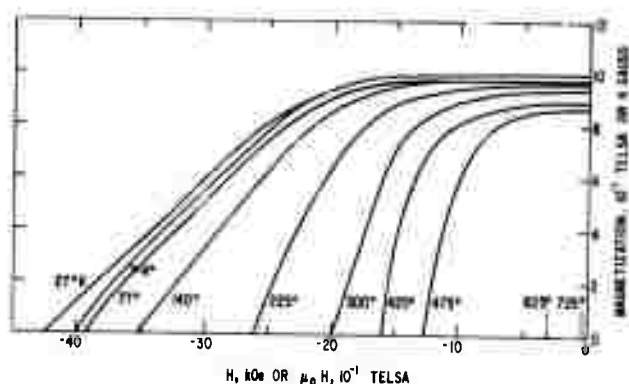


Fig. 1 Variation of demagnetization characteristics of a Co-Sm magnet with measurement temperature.

\*This work was supported in part by the Advanced Project Agency of the Department of Defense and was monitored by the Air Force Materials Laboratory, MAYE, under Contract F33615-70-C-1626.

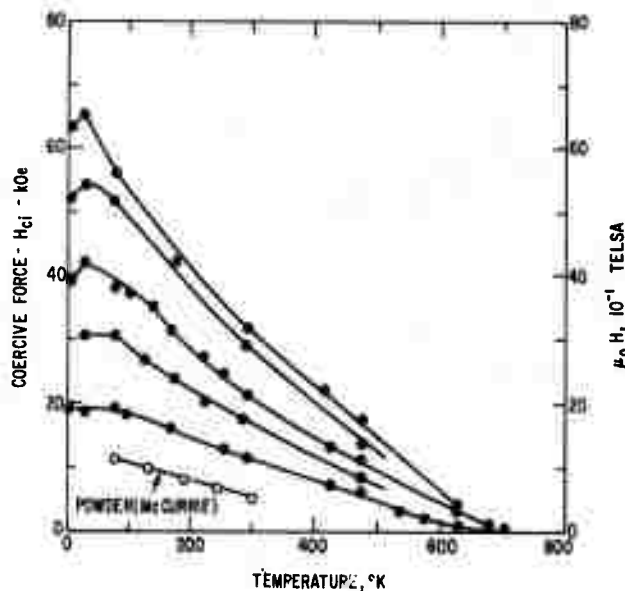


Fig. 2 Change of intrinsic coercive force with temperature for a series of Co-Sm magnet samples. The data for the powder are from McCurrie.<sup>(2)</sup>

was altered by varying the samarium composition slightly or by use of different post-sintering heat treatments.<sup>(8)</sup> Results by McCurrie<sup>(2)</sup> for  $\text{Co}_5\text{Sm}$  powder (particle size less than  $20\mu$ ) are included for comparison. Several features stand out:

1. The highest value of  $H_{ci}$  measured was 65 kOe. This value is a substantial fraction of the anisotropy field [estimated to be about 200 kOe at  $0^\circ\text{K}$  from data given by Tatsumoto et al.<sup>(9)</sup>]; however, as pointed out by McCurrie,<sup>(2)</sup> at the  $H_{ci}$  point where the net magnetization is zero, only half the volume of the sample has been reversed. Still higher fields are required to reverse the magnetization of all the particles; therefore, many particles in the sample had  $H_{ci}$  values  $\gg 65$  kOe.

2. The coercivity for all the samples drops to zero at about  $700^\circ\text{K}$ .

3. Below  $100^\circ\text{K}$  the coercivity of some of the samples peaks near  $27^\circ\text{K}$  and then drops slightly; and in others only small changes occur with temperature.

It is interesting to note that when these data are normalized to the  $H_{ci}$  measured at  $77^\circ\text{K}$ , the points for all the samples fall on the same curve as shown in Fig. 3. From this we conclude:

1. Factors which influence the magnitude of  $H_{ci}$  at any temperature do not influence the relative change of coercivity with temperature.

2. Structural factors giving rise to a high intrinsic coercive force are most effective at low temperatures and least effective at high temperatures.

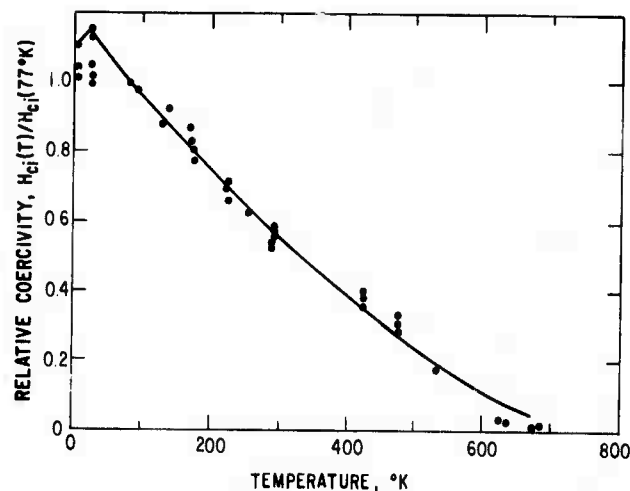


Fig. 3 Relative coercivity vs temperature. The data in Fig. 2 have been normalized so that the relative coercivity at  $77^\circ\text{K}$  is 1.

The temperature dependence of coercivity for Co-Sm magnets appears to correlate best with observations by Westendorp<sup>(4)</sup> regarding the change in domain wall energy with temperature.

#### ACKNOWLEDGMENTS

The authors wish to thank J. Geersten, R. Kopp, R. Laing, W. Moore, and A. C. Rockwood for their assistance in the preparation and testing of the samples; also R. J. Charles and J. D. Livingston for interesting technical discussions.

#### REFERENCES

1. W. A. J. J. Velge and K. H. J. Buschow, "Permanent Magnetic Properties of Rare Earth Cobalt Compounds ( $\text{RCO}_5$ )," Proc. IEE Conf. on Magnetic Materials and Their Applications, London, Sept. 1967, pp. 44-50.
2. R. A. McCurrie, "Determination of Intrinsic Coercivity Distributions in Aligned Assemblies of Uniaxial  $\text{SmCo}_5$  and  $\text{LaCo}_5$  Particles," Phil. Mag. 22, No. 179, 1013-1023 (1970).
3. R. A. McCurrie and G. P. Carswell, "Magnetic Hardness of the Intermetallic Compound  $\text{SmCo}_5$  as a Function of Particle Size," Phil. Mag. 23, 333 (1971).
4. D. L. Martin and M. G. Benz, "Magnetization Changes for Cobalt-Rare Earth Permanent Magnet Alloys When Heated up to  $650^\circ\text{C}$ ," IEEE Trans., MAG-8, 35 (March 1972).
5. F. F. Westendorp, "Domains in  $\text{SmCo}_5$  at Low Temperature," Conference on Magnetism and Magnetic Materials, Chicago, Paper 3F-2 (Nov. 1971).

6. P. Gaunt, "Domain Wall Pinning as a Source of Magnetic Hardening in Alloys," J. Appl. Phys. 43, 637 (1972).
7. M. G. Benz and D. L. Martin, "Measurement of Magnetic Properties of Cobalt-Rare Earth Permanent Magnets," IEEE Trans., MAG-7, 285-291 (1971).
8. M. G. Benz and D. L. Martin, "Cobalt-Mischmetal-Samarium Permanent Magnet Alloys: Process and Properties," J. Appl. Phys., 42, 2786-2789 (1971).
9. E. Tatsumoto, T. Okamoto, H. Fujii, and C. Inoue, "Saturation Magnetic Moment and Crystalline Anisotropy of Single Crystals of Light Rare Earth Cobalt Compounds  $RCO_5$ ," J. Physique 32, C1, 550-551 (1971).

# ANISOTROPY PARAMETERS AND COERCIVITY FOR SINTERED $\text{Co}_5\text{Sm}$ PERMANENT MAGNET ALLOYS

M.G. Benz and D.L. Martin  
General Electric Company  
Corporate Research and Development  
Schenectady, New York 12301  
(Submitted to Applied Physics Letters)

## INTRODUCTION

Previous efforts to understand the irreversible losses observed for cobalt-rare earth permanent magnets demonstrated that these losses are best understood by measurement of a series of demagnetization curves at the temperatures of interest.<sup>(1)</sup> The dominant feature of such a family of curves is the very large temperature dependence of intrinsic coercive force  $H_{ci}$ . Examination of a variety of cobalt samarium samples with large differences in  $H_{ci}$  (-12 kOe to -33 kOe at 300°K) showed them to have a common response of relative coercivity to temperature, as given in Fig. 1.<sup>(2)</sup>

In this study; saturation magnetization  $4\pi J_s$ , intrinsic coercive force  $H_{ci}$ , anisotropy field  $H_A$ , anisotropy constants  $K_1$ ,  $K_2$  and domain wall energy  $\gamma$  were determined for a single sample of sintered  $\text{Co}_5\text{Sm}$  at temperatures between 4.2°K and 500°K, in order to see if the temperature dependence of relative coercivity could be related to the temperature dependence of the anisotropy parameters and wall energy.

## SAMPLE PREPARATION

A highly aligned polycrystalline sample of  $\text{Co}_5\text{Sm}$  was prepared by the multiphase sintering approach outlined previously.<sup>(3)</sup> From this cylindrical sample (7.5 mm diameter  $\times$  2.5 cm long); a cube, 3.2 mm on edge, was cut such that one principle axis of the cube was parallel to the alignment direction

of the original cylinder and hence parallel to the hexagonal axes of the  $\text{Co}_5\text{Sm}$  grains. This principle axis of the sample will be referred to as the c-axis. From density measurements and chemical analysis, this sample was estimated to consist of 8 volume % voids, 3.2 volume %  $\text{Sm}_2\text{O}_3$  (2.8 wt %), and 88.8 volume %  $\text{Co}_5\text{Sm}$  with an average composition of 16.7 at % Sm. The  $\text{Co}_5\text{Sm}$  contained a trace amount of  $\text{Co}_7\text{Sm}_2$  as indicated by metallography and x-ray measurement of the lattice parameter. The lattice parameters  $c = 3.970 \pm 0.001\text{\AA}$  and  $a = 5.002 \pm 0.001\text{\AA}$  were similar to those previously observed for  $\text{Co}_5\text{Sm}$  in equilibrium with the  $\text{Co}_7\text{Sm}_2$  phase.<sup>(4)</sup> The grain size for the sintered grains was between 5 and 10  $\mu\text{m}$ . At room temperature this sample had a magnetization at 100 kOe of 9.35 kGauss; a remanent magnetization of 8.93 kGauss, an open circuit magnetization of 8.16 kGauss at a field of -1.99 kOe; and an intrinsic coercive force of -30.5 kOe. The magnetic alignment factor, estimated by dividing the remanent magnetization by the magnetization at 100 kOe, was 0.96. The shape dependent demagnetizing field, opposing the applied field for these measurements, was estimated by means of the polar radiation model<sup>(5)</sup> to be  $0.244 \times 4\pi\text{J}$ .

## SAMPLE MEASUREMENT

The magnetization of the sample was measured parallel and perpendicular to the c-axis by the ballistic method for small samples outlined previously.<sup>(1)</sup>

The applied field was provided by a superconducting solenoid. The 4.2°K and 77°K measurements were made at the boiling points of liquid helium and liquid nitrogen, respectively. The 500°K measurement was made with the sample heated by a small electric furnace which fitted inside the superconducting solenoid system.

The sequence used for the measurements at each temperature was as follows: 1) Magnetize the sample parallel to the c-axis at 300°K. 2) Measure the magnetization of the sample parallel to the c-axis at the temperature  $T$  ( $T = 4.2$  , 77 , 300 , or 500°K). 3) Re-magnetize the sample parallel to the c-axis at 300°K. 4) Measure the magnetization of the sample perpendicular to the c-axis at the temperature  $T$  as a function of increasing field.

## RESULTS

With the magnetizing field parallel to the c-axis, the magnetization of the sample was measured in the direction of the c-axis in order to determine  $4\pi J_S$ . The values for  $4\pi J_S$  were taken as the values for  $4\pi J$  measured at 100 kOe at 4.2, 77 , and 300°K; and the value measured at 60 kOe at 500°K. These values are listed in Table I.

With the demagnetizing field parallel to the c-axis, the magnetization of the sample was measured in the direction of the c-axis in order to determine  $H_{ci}$ . These values are also listed in Table I.

With the magnetizing field perpendicular to the c-axis, the magnetization of the sample was measured in the direction of the magnetizing field as a function of increasing field. These data are shown in Fig. 2. The 4.2°K data are plotted separately to show the low field nonlinear portion of the curve. This effect is unexplained, but shows the necessity of fields approaching 100 kOe and above for this type of measurement.

As discussed by Sucksmith and Thompson,<sup>(6)</sup> when the magnetizing field is perpendicular to the c-axis, the saturation magnetic moment per unit

volume  $J$  measured in the direction of the magnetizing field is given by the expression:

$$J_s H = 2K_1 \left( \frac{J}{J_s} \right) + 4K_2 \left( \frac{J}{J_s} \right)^3 \quad (1)$$

Here  $K_1, K_2$  are the anisotropy constants,  $J_s$  is the saturation magnetic moment per unit volume, and  $H$  is the effective magnetizing field perpendicular to the  $c$ -axis. By rearrangement:

$$\frac{H}{J} = \frac{2K_1}{J_s^2} + \frac{4K_2}{J_s^4} J^2 \quad (2)$$

Hence, a plot of  $H/J$  vs  $J^2$ , as given in Fig. 3, can be used to determine  $2K_1/J_s^2$  from the intercept and  $4K_2/J_s^4$  from the slope. Values for  $2K_1/J_s^2$  taken from this figure are listed in Table I. The slope  $4K_2/J_s^4$  was considered to be equal to zero for these plots.

Using the above data, values for the anisotropy field  $H_A$ , the anisotropy constant  $K_1$  and the domain wall energy  $\gamma$  were calculated by use of the expressions:

$$H_A = \left( \frac{4\pi J_s}{4\pi} \right) \left( \frac{2K_1}{J_s^2} \right) \quad (3)$$

$$K_1 = \frac{1}{2} \left( \frac{4\pi J_s}{4\pi} \right)^2 \left( \frac{2K_1}{J_s^2} \right) \quad (4)$$

$$\gamma = (2k T_c K_1/d)^{1/2} \quad (5)$$

Here  $k$  is Boltzmann's constant,  $T_c$  is the Curie temperature (984°K from Ref. 7), and  $d$  is the distance between magnetic atoms<sup>(8)</sup> (taken as equal to one half of the  $a$  lattice parameter). These values were also listed in Table I.

The upper half of Table I is calculated on the basis of the total sample;

8 volume % voids, 3.2 volume %  $\text{Sm}_2\text{O}_3$  and 88.8 volume %  $\text{Co}_5\text{Sm}$ . The

lower half of the table is calculated on the basis of 100 volume %  $\text{Co}_5\text{Sm}$ .

## DISCUSSION

The values for  $4\pi J_s$  and  $H_{ci}$  measured for this sample are in agreement with previous values presented by the authors. <sup>(2, 9)</sup>

The values for anisotropy field  $H_A$  and the anisotropy constant  $K_1$  at 300°K are in good agreement with data for single crystals presented by Strnat, <sup>(10)</sup> Buschow, <sup>(11)</sup> and Tatsumoto et al. <sup>(7)</sup> A much different temperature dependence is observed, however. This may be due to the polycrystalline nature of the sample used for this study, differences in composition, or the higher fields used for these measurements.

Accepting the temperature dependence of anisotropy field, anisotropy constant, and domain wall energy presented here; the most striking aspect of the results presented in Table I is the similarity between the temperature dependence of these anisotropy parameters and the temperature dependence of  $H_{ci}$ . As indicated in Figs. 4-6, these data support models for relating coercivity directly to the anisotropy constant [ Fig. 4]; or models relating coercivity to the anisotropy field as advanced by McCurrie <sup>(12)</sup> [ Fig. 5]; or models relating coercivity to the domain wall energy ( $\gamma/J_s$  actually) as advanced by Zijlstra <sup>(8)</sup> and Westendorp <sup>(13, 14)</sup> [ Fig. 6]. This later model is only supported by the data if the model is modified to include the concept that  $H_{ci}$  drops to zero at some finite value of  $\gamma/J_s$  (viz. 0.0275 erg/G·cm<sup>2</sup>). Which of these models truly describes the case at hand is yet to be firmly established.

An attempt was also made to relate the above to the classical temperature dependence of magnetic anisotropy presented by Zener.<sup>(15)</sup> As illustrated in Fig. 7, it was found that the relationship had to be modified in a manner similar to the work of Carr for hexagonal cobalt<sup>(16)</sup> in order to fit the data.

#### ACKNOWLEDGMENTS

The authors would like to acknowledge the assistance of W. F. Moore in preparation of the alloys; R. W. Kopp in the design of measurement equipment; J. T. Geertsen, R. T. Laing, R. P. Laforce, and A. C. Rockwood in the preparation and magnetic measurement of the sample; and W. E. Balz and R. Goehner for the chemical and x-ray analysis.

In addition, the authors would like to acknowledge the assistance of J. J. Becker and J. D. Livingston for the many helpful discussions during this study.

This work was sponsored, in part, by the Advanced Research Projects Agency, under the direction of the Air Force Materials Laboratory, Wright-Patterson Air Force Base, Ohio, Contract F33615-70-C-1626.

## References

1. D.L. Martin and M.G. Benz, "Magnetization Changes for Cobalt-Rare Earth Permanent Magnet Alloys When Heated Up to 650°C," IEEE Trans. Magn. MAG-8, 35 (1972).
2. D.L. Martin and M.G. Benz, "Temperature Dependence of Coercivity for Co-Sm Permanent Magnet Alloys," Proc. International Magnetism Conference, Kyoto, Japan, April 10-13, 1972, IEEE Trans. Magn. MAG-8, Sept. (1972).
3. M.G. Benz and D.L. Martin, "Cobalt-Samarium Permanent Magnets Prepared by Liquid Phase Sintering," Appl. Phys. Letters 17, 176 (1970).
4. M.G. Benz and D.L. Martin, unpublished.
5. R.J. Parker and R.J. Studders, Permanent Magnets and Their Application, John Wiley and Sons, Inc., New York, pp 163-168 (1962).
6. W. Sucksmith and J.E. Thompson, "The Magnetic Anisotropy of Cobalt," Proc. R. Soc. 225, 362 (1954).
7. E. Tatsumoto, T. Okamoto, H. Fujii, and C. Inoue, "Saturation Magnetic Moment and Crystalline Anisotropy of Single Crystals of Light Rare Earth Cobalt Compounds  $RCo_5$ ," Supplement J. de Physique 32, C1-550 (1971).
8. J. Zijlstra, "Domain-Wall Processes in  $SmCo_5$  Powders," J. Appl. Physics 41, 4881 (1970).
9. S. Foner, E.J. McNiff, Jr., D.L. Martin, and M.G. Benz, "Magnetic Properties of Cobalt-Samarium with a 24 MGOe Energy Product," General Electric Company TIS Report 72-CRD-073, submitted to Appl. Phys. Letters.

10. K. Strnat, "The Recent Development of Permanent Magnet Materials Containing Rare Earth Metals," IEEE Trans. Mag. MAG-6, 182 (1970).
11. K.H.J. Buschow and W.A.J.J. Velge, "Permanent Magnetic Materials of Rare Earth Cobalt Compounds," Z. angew. Phys. 26, 157 (1969).
12. R.A. McCurrie, "Determination of Intrinsic Coercivity Distributions in Aligned Assemblies of Uniaxial  $\text{SmCo}_5$  and  $\text{LaCo}_5$ ," Phil. Mag. 22, 1013 (1970).
13. F.F. Westendorp, "Domain-Wall Energy and Coercive Force of Cobalt Rare-Earth Permanent Magnet Materials," J. Appl. Phys. 42, 5727 (1971).
14. F.F. Westendorp, "Domains in  $\text{SmCo}_5$  at Low Temperature," to be published - Applied Physics Letters.
15. C. Zener, "Classical Theory of Temperature Dependence of Magnetic Anisotropy Energy," Phys. Rev. 96, 1335 (1954).
16. W.J. Carr, Jr., "Temperature Dependence of Ferromagnetic Anisotropy," Phys. Rev. 109, 1971 (1958).

TABLE I

Magnetization and Anisotropy Data for Sintered  $\text{Co}_5\text{Sm}$ 

Basist†	T °K	$4\pi J_s$ kG	$H_{ci}$ kOe	$2K_1/J_s^2$ Oe/G	$H_A$ kOe	$K_1^*$ $10^7$ erg/cm <sup>3</sup>	$\gamma$ erg/cm <sup>2</sup>
	4.2	10.0	-52.0	530			
Sample	77	9.88	-52.7	570			
	300	9.35	-30.5	385			
	500	8.53	-16.7	250			
$\text{Co}_5\text{Sm}$	4.2	11.2	-52.0	472	421	18.9	45.3
	77	11.1	-52.7	507	448	19.8	46.4
	300	10.5	-30.5	343	286	11.9	35.9
	500	9.58	-16.7	223	170	6.47	26.5

†The values listed on a sample basis are those actually measured for the sample as a whole. The values listed on a  $\text{Co}_5\text{Sm}$  basis are those the sample would have if it were 100 volume %  $\text{Co}_5\text{Sm}$  instead of 88.8 volume %  $\text{Co}_5\text{Sm}$ .

\*1 G·Oe = 1 erg/cm<sup>3</sup>.

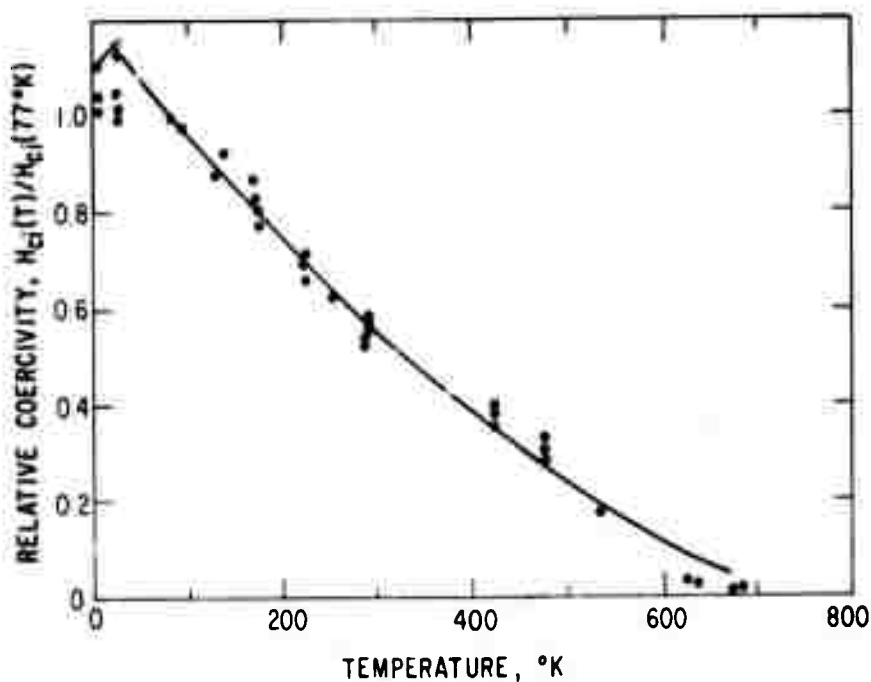


Fig. 1 Relative coercivity vs temperature. The data were normalized so that the relative coercivity at 77°K was equal to 1.

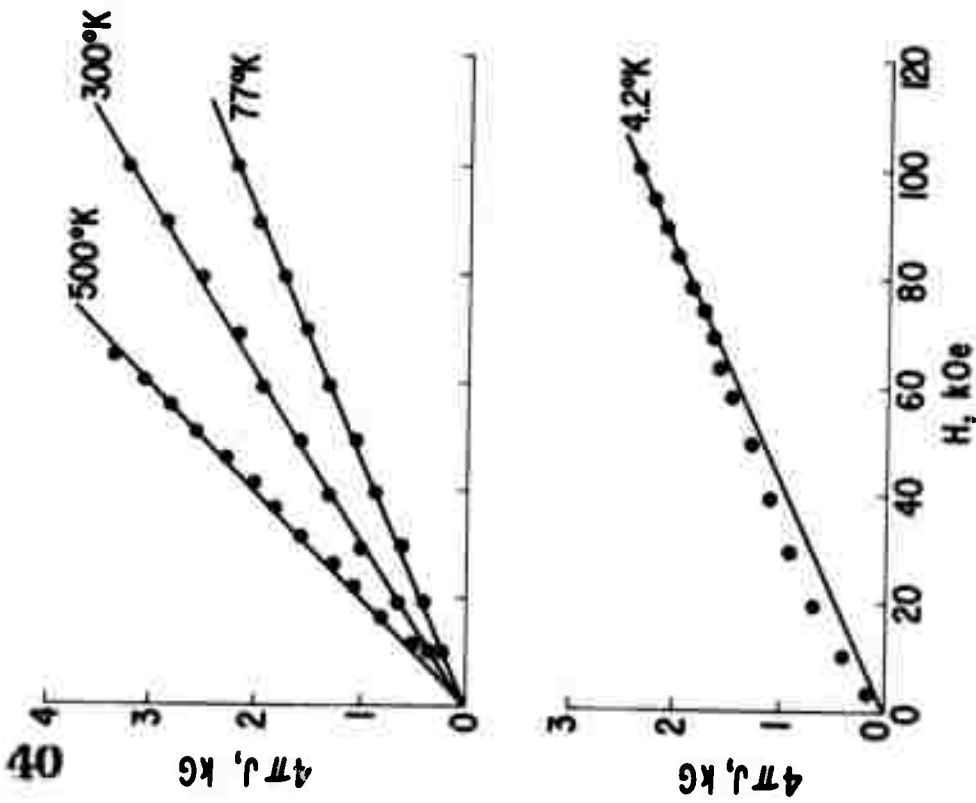


Fig. 2 Magnetization of the sample measured perpendicular to the c-axis as a function of field applied perpendicular to the c-axis.

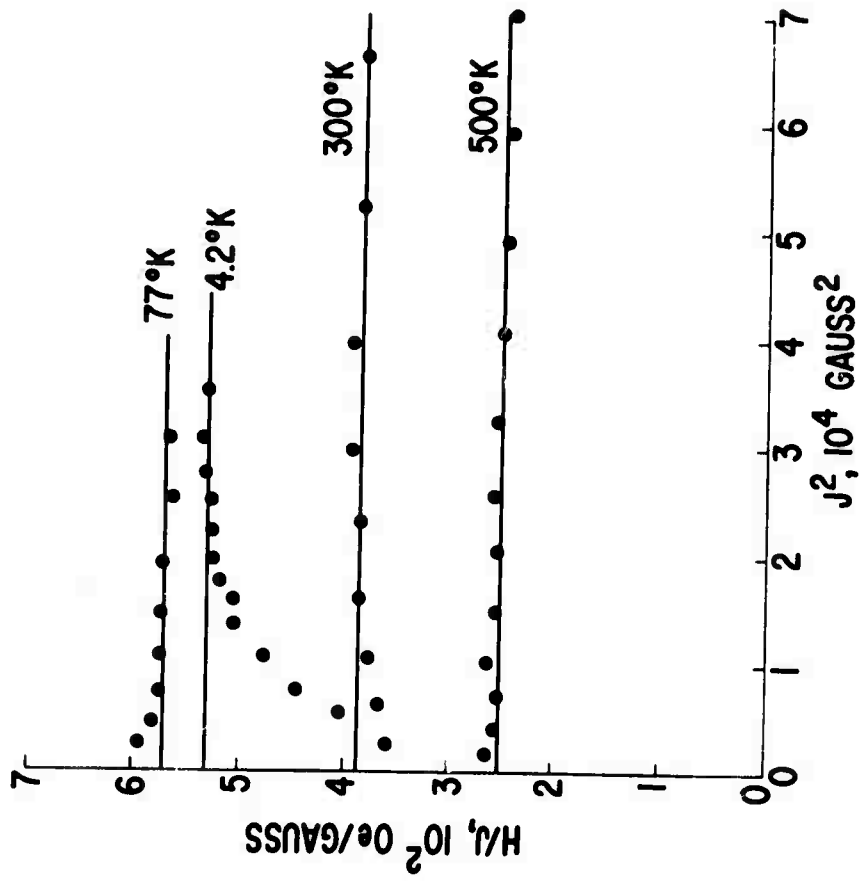


Fig. 3  $H/J$  vs  $J^2$ . The intercept is equal to  $2K_1/J_S^2$ .

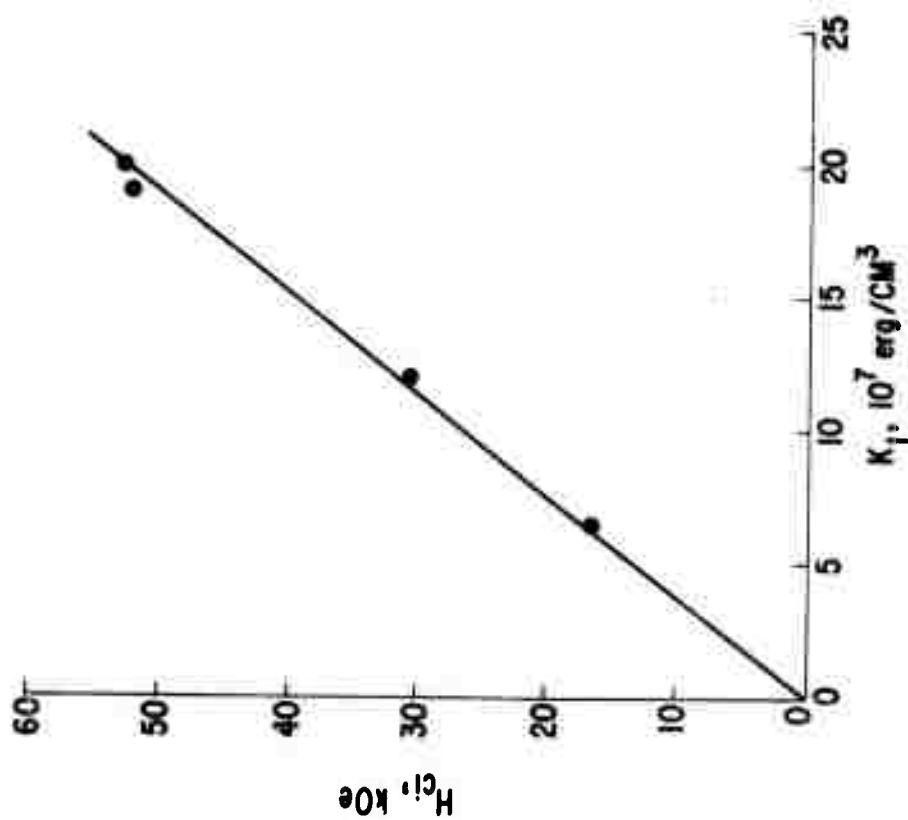


Fig. 4  $H_{ci}$  vs the anisotropy constant  $K_1$ .

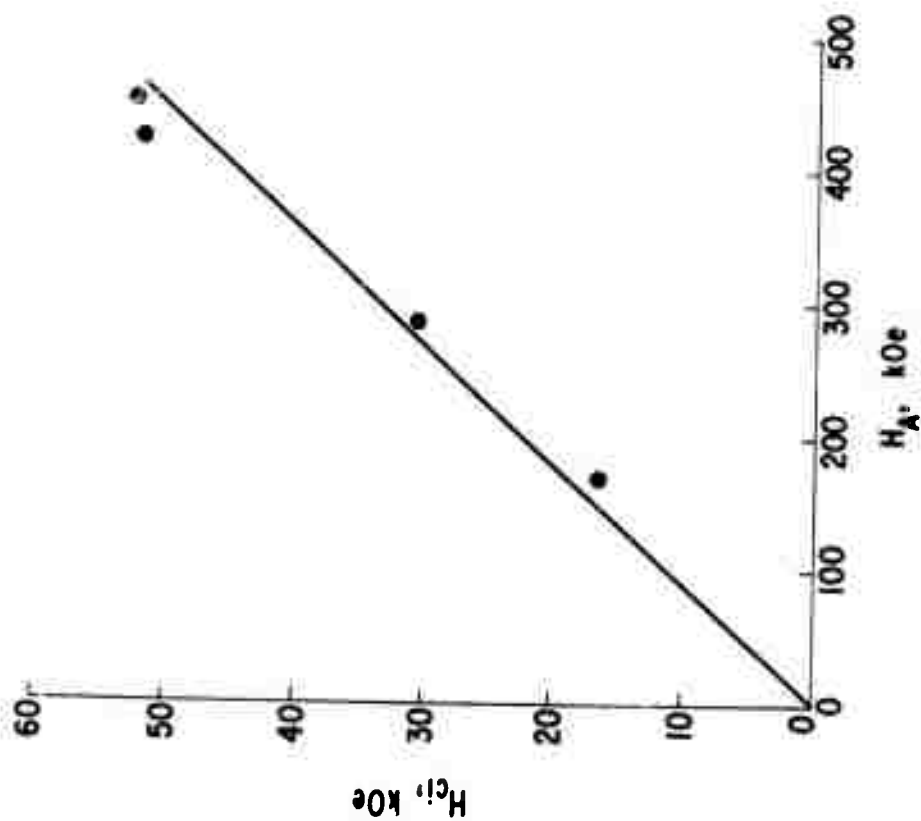


Fig. 5  $H_{ci}$  vs the anisotropy field  $H_A$ .

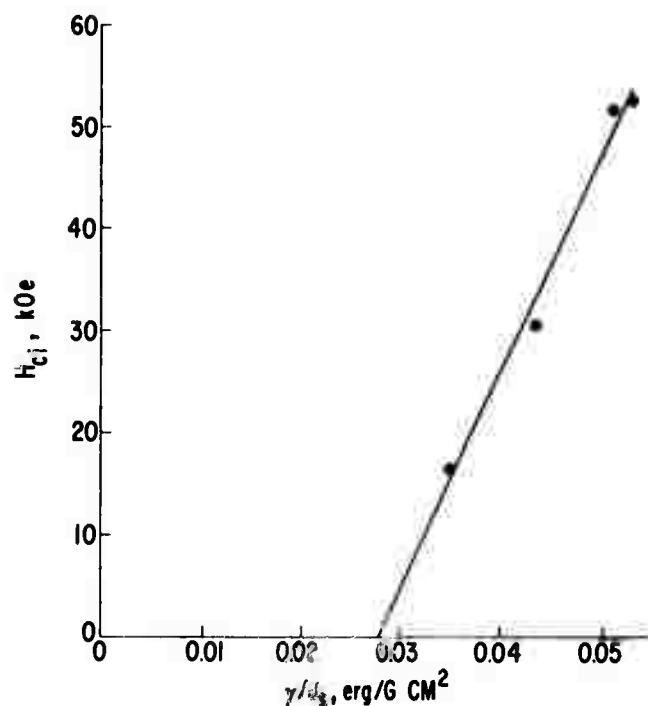


Fig. 6  $H_{ci}$  vs the domain wall energy  $\gamma$  divided by the saturation magnetic moment per unit volume  $J_s$ .

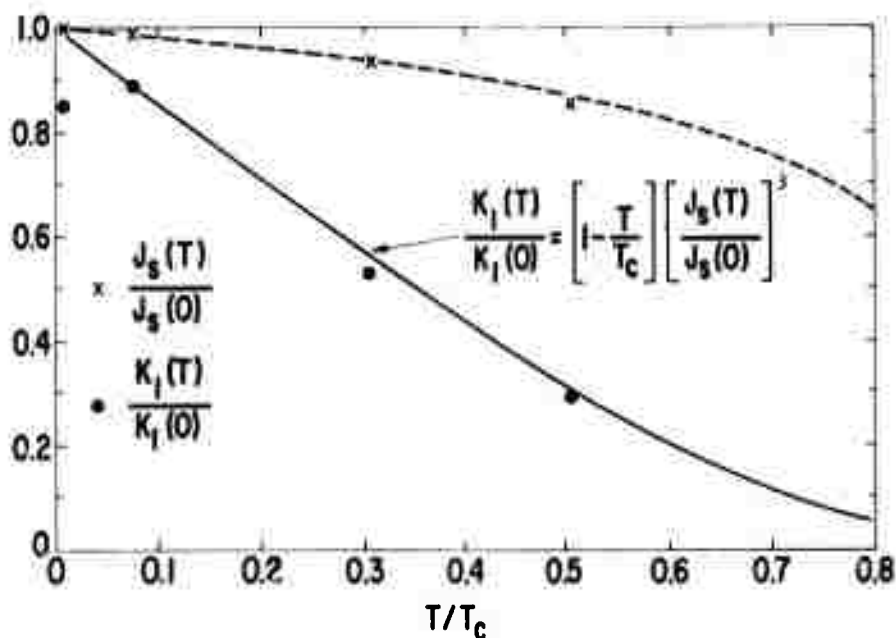


Fig. 7  $J_s(T)/J_s(0)$  and  $K_1(T)/K_1(0)$  as a function of  $T/T_c$ .  $J_s(0)$  was taken as the value for  $J_s$  at 4.2°K.  $K_1(0)$  was taken as  $K_1(77^\circ\text{K})/0.889$ , the value 0.889 being  $[1 - T/T_c][J_s(T)/J_s(0)]^3$  at  $T = 77^\circ\text{K}$ . The solid curve was calculated by placing the empirically determined Carr<sup>(16)</sup> type factor  $(1 - T/T_c)$  into the Zener<sup>(15)</sup> equation.  $T_c$  was taken as 984°K. (7)